NASA/TM-20260000121

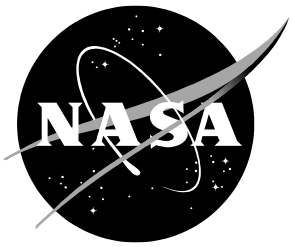

Combined Test and Analysis Approach to Develop Energy Absorbing Systems for eVTOL Aircraft

Jacob B. Putnam, Justin D. Littell, Nathaniel W. Gardner, Robin C. Hardy, Matlock Mennu
Langley Research Center, Hampton, Virginia

January 2026

Since its founding, NASA has been dedicated to the advancement of aeronautics and space science. The NASA scientific and technical information (STI) program plays a key part in helping NASA maintain this important role.

The NASA STI program operates under the auspices of the Agency Chief Information Officer. It collects, organizes, provides for archiving, and disseminates NASA's STI. The NASA STI program provides access to the NTRS Registered and its public interface, the NASA Technical Reports Server, thus providing one of the largest collections of aeronautical and space science STI in the world. Results are published in both non-NASA channels and by NASA in the NASA STI Report Series, which includes the following report types:

- TECHNICAL PUBLICATION. Reports of completed research or a major significant phase of research that present the results of NASA Programs and include extensive data or theoretical analysis. Includes compilations of significant scientific and technical data and information deemed to be of continuing reference value. NASA counterpart of peer-reviewed formal professional papers but has less stringent limitations on manuscript length and extent of graphic presentations.

- TECHNICAL MEMORANDUM. Scientific and technical findings that are preliminary or of specialized interest, e.g., quick release reports, working papers, and bibliographies that contain minimal annotation. Does not contain extensive analysis.

- CONTRACTOR REPORT. Scientific and technical findings by NASA-sponsored contractors and grantees.

- CONFERENCE PUBLICATION. Collected papers from scientific and technical conferences, symposia, seminars, or other meetings sponsored or co-sponsored by NASA.

- SPECIAL PUBLICATION. Scientific, technical, or historical information from NASA programs, projects, and missions, often concerned with subjects having substantial public interest.

- TECHNICAL TRANSLATION. English-language translations of foreign scientific and technical material pertinent to NASA's mission.

Specialized services also include organizing and publishing research results, distributing specialized research announcements and feeds, providing information desk and personal search support, and enabling data exchange services.

For more information about the NASA STI program, see the following:

- Access the NASA STI program home page at http://www.sti.nasa.gov

- Help desk contact information:

https://www.sti.nasa.gov/sti-contact-form/
and select the "General" help request type.

NASA/TM-20260000121

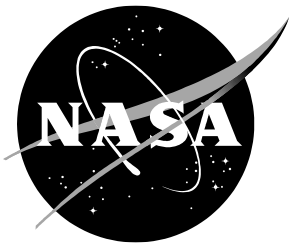

Combined Test and Analysis Approach to Develop Energy Absorbing Systems for eVTOL Aircraft

Jacob B. Putnam, Justin D. Littell, Nathaniel W. Gardner, Robin C. Hardy, Matlock Mennu
Langley Research Center, Hampton, Virginia

National Aeronautics and
Space Administration

Langley Research Center
Hampton, Virginia 23681-2199

January 2026

Available from:

NASA STI Program / Mail Stop 050
NASA Langley Research Center
Hampton, VA 23681-2199

NASA STI Program Report Series

Table of Contents

Table of Figures

1 Abstract

Researchers at the National Aeronautics and Space Administration (NASA) have developed novel energy absorbing (EA) components as example technologies which aim to provide insights into methods and techniques for improving occupant safety within electric Vertical Take-off and Landing (eVTOL) vehicles. An EA component design approach was matured. This design approach utilizes a combination of test and analysis methods to generate and refine EA component designs and to verify their capability from sub-scale to full-scale integration within representative vehicle structures. Through these efforts, lightweight seat and subfloor EA technologies were developed and their capability to improve occupant safety in relevant loading environments were demonstrated. The developed methodology, EA component designs, and demonstrated capability are reported within this TM with the goal of improving occupant protection design within future eVTOL vehicles.

2 Introduction

Advancements in electric propulsion and lightweight materials for aerospace structures have opened the door for a new technological development race in the form of electric Vertical Take-off and Landing (eVTOL) vehicles. These vehicles promise to open new avenues of aerospace transportation, particularly within urban environments in which flights using traditional aerospace transportation methods have been limited by noise and logistics issues. Currently there are over 200 eVTOL vehicle concepts, in various stages of design and production, competing for early entry into this market. These new vehicle designs utilize non-typical materials, structural designs, and propulsion methods to overcome weight limitations associated with current electric propulsion technology and expected operational environments. Though this has produced a plethora of new vehicle designs which do not conform to traditional general aviation (GA) or rotorcraft designs there are several consistent design features which have emerged. The driving criteria of eVTOL design, to minimize vehicle weight, has produced designs with reduced vehicle structure around the occupant and structures which are composed of lightweight carbon-fiber composites rather than typical metallic materials. Unfortunately, reducing the structural volume around the occupant compartment limits the amount of impact energy which can be absorbed by the vehicle during any form of dynamic impact. Though the high strength to weight ratio carbon-fiber provides many benefits for aerospace structural designs, it's low ductility makes it a poor performer for absorbing impact energy. The absorption of impact energy by vehicle structure is an essential component of crashworthy design used by automotive and aerospace industries to reduce loads transferred to occupants during a crash. With two of the most common features of current eVTOL aircraft designs working against their ability to effectively absorb impact energy in a crash environment, manufacturers will need energy absorbing (EA) design solutions, independent from the vehicle structure, to meet crashworthiness standards.

The development of novel EA components to improve crashworthiness in aerospace vehicles has been an area of continuous research at NASA's Langley Research Center in Hampton, Virginia. Previous research in this field has included the development of EA systems ranging from deployable honeycomb structures [1] to conusoidal composite keel beams [2]. This work has led to a wealth of knowledge in the interplay between material, geometry, and impact environment on the effectiveness of EA components within

aerospace structures. The current study aims to leverage this knowledge to develop a systematic approach for designing EA components to improve crashworthiness capabilities.

3 Methods

3.1 Approach Overview

A multistep process utilizing test and analytical methods was used to develop, optimize, and demonstrate advanced EA components for the improvement of aerospace occupant safety. The first step of this approach was to define design criteria for the EA components. The first criteria was that the EA systems needed to reduce peak accelerative force transferred through the vehicle to a seated occupant to levels which reduced occupant injury risk to rates below those defined in current aerospace crashworthiness requirements. The FAA requirements for emergency landing conditions for normal aircraft and rotorcraft limits the peak lumbar spine force for a 50th percentile male occupant to 1500 lbs [3,4]. Next the EA systems were to be designed to optimize energy absorbing efficiency. Optimal energy absorbing efficiency can be quantified as the energy absorbed by the structure relative to the peak accelerative force transferred through it. An example of optimal energy absorption compared to inefficient energy absorption measured by impact acceleration over time is shown in Figure 1. The optimal EA system produces a near square acceleration profile with a steady state acceleration during the energy absorption phase equal to the accelerative force required for initiation. The poor EA system requires higher accelerative force for initiation than it produces during the energy absorption phase resulting in higher loads transferred to the occupant for the same amount of impact energy. The final two design criteria focused on improving capability with respect to the unique design challenges of eVTOL vehicles. As eVTOL vehicles are currently limited by weight restrictions the third design goal was to reduce the EA system weight as much as possible. Lastly the EA systems were designed to be self-supporting, meaning they were not to be reliant on the vehicle structure for their effectiveness. To make the EA systems applicable across a wide range of vehicle shapes, sizes, and functions they had to be designed independent from the vehicle structure.

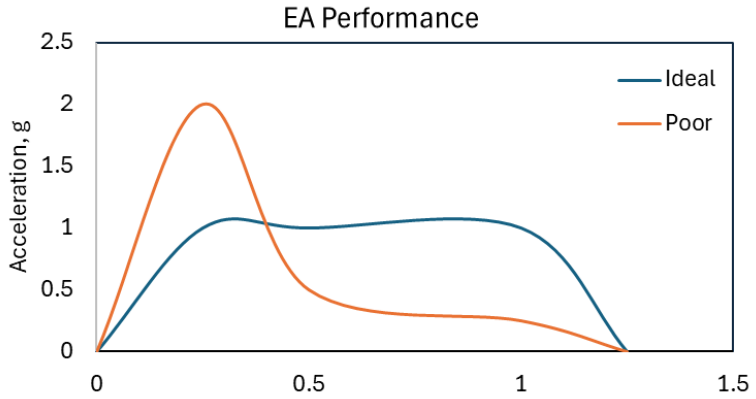

Figure 1. Comparison of notional energy absorbing efficiency in an ideal and poor EA design.

The design criteria selected for the EA systems can be summarized as follows: reduce accelerative loads below current aerospace certification criteria limits, produce optimal energy absorbing efficiency, limit component weight, and be self-supporting. These criteria were set out to be achieved through material selection and optimization of the EA design geometry. Several different test facilities were used at NASA Langley to quantify material system properties, quantify component level design responses, and verify system level capabilities. Throughout the process analytical models were utilized to explore the initial design space, optimize design geometries, and expand the assessment of system level capabilities. The test facilities utilized in this effort as well as the analytical tools used are discussed in the following sections.

3.2 Test Facilities

All testing conducted during the EA component development process was carried out using facilities housed by the Structural Dynamics Branch at NASA Langley. Quasi-static material characterization tests of coupon samples were conducted using an electromechanical universal testing machine, MTS Criterion Model 43, equipped with a 10,000 lb load cell. For each material characterization test, specimens were first spray painted with a white base coat and then a high-contrast black speckle pattern was applied for low-speed three-dimensional digital image correlation (3D-DIC). A pair of 5-megapixel (MP) cameras were positioned in front of the test fixture to capture images at 1 Hz. Real-time monitoring was conducted using VIC-3D, a commercially available software through Correlated Solutions, Inc. Virtual extensometers were placed within the field-of-view to measure specimen strain during the loading. Strain values measured by DIC were used to compare with and verify the strain measured by the MTS test machine. An image showing a typical coupon material characterization test (static, tensile), along with a typical speckle coated test coupon, is provided in **Error! Reference source not found.**.

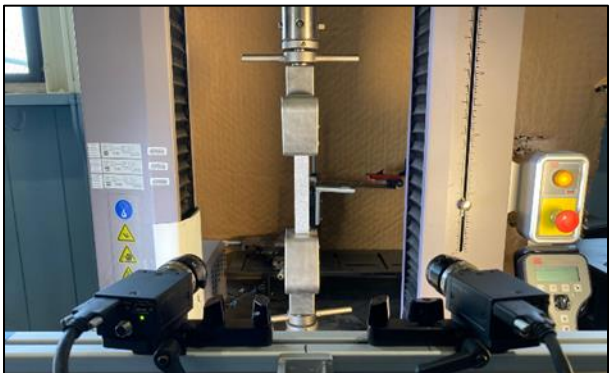

Figure 2. Coupon material characterization test setup.

Two drop towers were used to conduct component and sub-system level characterization testing (dynamic, compression). For testing of the individual EA component designs, a configurable 15-ft drop tower was used. Drop height and mass were adjusted to produce the desired impact energy and speeds. For sub-system level testing which included both seat level and stacked EA system, a larger 30-ft drop tower was used. In this tower, the sub-system was mounted to a drop mass and dropped onto a pulse generating material from varying heights in order to apply specific impact acceleration pulses into the sub-system. The drop height, drop mass, and pulse generating material were all adjustable to create specific impact velocities, energies, and acceleration shapes. In both drop towers, high-speed photogrammetry was utilized to capture EA system mechanics during the test event. Images of the 15- and 30-ft drop towers are provided in Figure 3. A full-scale vehicle test was conducted in order to verify the response of the developed EA components

Figure 3. Drop tower test facilities: 30 ft (left) and 15 ft (right).

within relevant multi-axis loading environments and in-situ aircraft structure. The full-scale vehicle tests were conducted at NASA Langley Landing and Impact Research (LandIR) Facility. An image of this test facility is provided in Figure 4. The LandIR facility consists of a 400 ft x 200 ft x 240 ft gantry structure which was originally designed as a simulation test bed for lunar landing vehicles. Since its original founding, the facility was retrofitted to test full-scale aircraft, rotorcraft, and spacecraft within dynamic loading environments. The facility uses a parallel winch system mounted at the top of the gantry tower to produce a controlled decent profile for each test article. Test articles can either be swung to produce multi-axis impact loads or dropped vertically. Historically, tests have included impacts into concrete, soil, or water surfaces. For the verification test performed on the developed EA systems, a representative eVTOL composite airframe was utilized in multi-axis impact swing tests. High-speed photogrammetry was used in these tests to track EA performance as well as 3D-DIC to measure full-field deformation and strain within the test article.

Figure 4. LandIR Test Facility.

3.3 Analysis Methodology

The non-linear dynamics solver software LS-Dyna (Ansys) was used to conduct computational analysis in support of EA component development and verification. Representative composite material models of each material system characterized for EA component development were generated using the *Mat_Laminated_Composite_Fabric (Mat_58) material model within LS-Dyna. Mat_58 is an anisotropic composite material model which allows the definition of quasi-static stress vs. strain response in each orthogonal material direction as well as strain-based damage and material failure criteria. The composite material layups used in the EA components were defined analytically using the *Part_Composite option within LS-Dyna which allows full composite layup to be defined by material, thickness, and orientation layer by layer all within a single element. A Belytschko-Tsay shell element formulation with Flanagan-Belytschko stiffness form hourglass control was generally used for the elements defined within each EA component model. Element formulation and hourglass control were selected based on best practices defined for moderate velocity impacts of composite material by the LS-Dyna aerospace working group [5]. The finite element model (FEM) mesh generating software Hypermesh (Altair) was used to generate geometries and FEM mesh for each EA component design. Hypermesh was also used for geometry parameterization in order to conduct geometry optimization analyses. The computational optimization software LS-OPT (Ansys) was used to conduct the geometry optimization analysis. All simulations were conducted on a Linux computer cluster. As this project occurred over a multi-year span, the LS-Dyna executable used evolved from Version R10.1 to R14.0 during the analyses conducted. The specific executable used for each portion of the analysis is described within each respective section of this report.

4 Material Characterization

4.1 Coupon Testing

The first step in developing an effective EA system for eVTOL vehicles was selecting an appropriate material for the design. The ideal material would need to be both ductile in order to effectively absorb energy within the crash environment and lightweight in order to minimize weight cost within eVTOL structural design. To meet these needs, hybrid woven composite fiber material systems were evaluated due to their exceptional weight to strength ratios, ability to be formed into complex shapes, and tunable levels of ductility through the selection of the fiber materials. Hybrid composite material systems consist of a combination of carbon and non-carbon fibers in a woven layup configuration. The carbon fibers typically are oriented in the warp direction while the non-carbon fibers are oriented in the fill direction. Accordingly, the directionality of the fibers gives the finished material orthotropic material properties. By designing to and optimizing the orthotropic nature of the material, desirable characteristics in both material stiffness and compliance can be achieved. For preliminary assessment, three composite fabric material systems were selected. The first was a traditional carbon plain weave, designated as C/C, which had carbon tows each containing 3,000 filaments (3k-sized) in both the warp and fill directions. The C/C material was used as a control rather than a true crushable design material. The second was a hybrid material, designated as C/K, consisted of plain weave 3k-sized carbon fibers in the warp direction and 3k-sized Kevlar fibers in the fill direction. This material is shown in . The third was also a hybrid material system, designated as C/U, which consisted of twill weave of 3k-sized carbon fiber in the warp direction and 3k-sized ultra-high molecular weight polyethylene (UHMWPE) material in the fill direction. A twill weave system was used for the C/U material system since a plain weave system was not available. In the initial material assessment, a West Systems (WS) 105 resin with 205 hardener resin system was used with each composite fabric. An image of the hybrid C/K material system is shown in Figure 5.

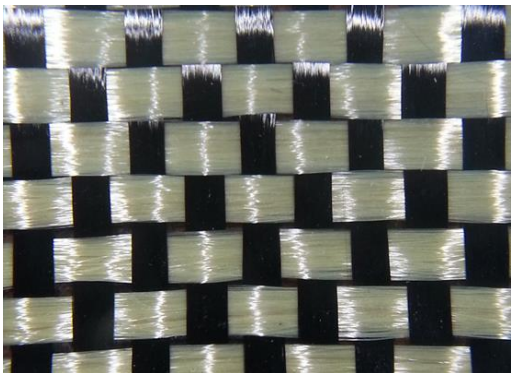

Figure 5. Hybrid C/K composite material system.

Baseline material properties were obtained for each selected material system through standardized coupon tests. Coupon specimens were fabricated for each material system by first laying up four-layer flat panels of each material and then curing them under vacuum. After curing, 1-in. wide by 10-in. long coupon specimens were cut from the sheet, where the orientation of the cut was adjusted to produce samples for warp, fill, and shear direction tests. Tests were conducted in both the warp and fill directions for the hybrid materials, C/K and C/U. Tensile tests were conducted in accordance to ASTM D3039 – Standard Test method for Tensile Properties of Polymer Matrix Composite Materials and in-plane shear tests were conducted in accordance to ASTM D3518 – Standard Test method for In-Plane Shear Response of Polymer Matrix Composite Materials by Tensile Test of a ±45° Laminate [7]. Specimens were tested in an electromechanical universal test machine at a quasi-static tensile rate of 0.1 in./min. Shear properties were determined from equations used to correlate axial data in the 45-degree direction to shear. The full set of material properties obtained from this testing can be found in [6]. An overview of the material properties obtained is reprinted in Table 1.

Table 1. Composite material properties

	Modulus (Msi)	**Ult. Strength (ksi)**	**Ult. Strain (in/in)**
Warp Direction			
C/C	6.5	76.3	0.011
C/K	6.3	77	0.013
C/U	5.4	56	0.011
Fill Direction			
C/C	6.5	76.2	0.011
C/K	2.8	54	0.025
C/U	2.6	67	0.033
Shear Direction			
C/C	0.79	17.4	0.20
C/K	0.45	3.1	0.45
C/U	0.33	8.3	0.15

Generally, all three material systems produced similar properties along the warp direction which was expected as each was composed of carbon fiber in this direction. The C/U material did exhibit slightly reduced modulus and ultimate strength along this direction which is associated with the fact that it was a twill fabric rather than plain weave. In the fill direction the carbon fiber in the C/C material exhibited the stiffest response, while the C/K material exhibited the lowest ultimate strength. The C/U material exhibited the lowest modulus and highest ultimate strain in the fill direction. In the shear direction the C/C material again exhibited the stiffest response, while the C/K material had the lowest ultimate strength, but significantly higher ultimate strains as compared to the other two materials. After quantifying the baseline properties of each material, they were then utilized in component level testing to identify their capability in EA systems.

4.2 Preliminary Component Testing

To evaluate the baseline EA capability of the three composite material systems, a component level dynamic impact test campaign was conducted. Flat walled crush-tube specimens were fabricated in-house at NASA Langley using a hand layup technique. Each test tube was fabricated with 4 layers of the respective fabric material and had a diameter of 3 in and a length of 6 in. The test tube specimens were subjected to vertical dynamic impact tests in which an instrumented drop mass was impacted onto the test specimen using the 15-ft drop tower at NASA Langley. In each test, a 102 lb. mass was dropped from a height of 6 feet, to achieve an impact velocity of approximately 20 ft/s. For each test, the bottom of the tube was rigidly fixed to the bottom of the drop tower while the top was left free. Acceleration of the drop mass was measured using a 500-g accelerometer with a recording rate of 10 kHz. A picture of a C/C crush tube specimen within the test environment can be seen in Figure 6.

.

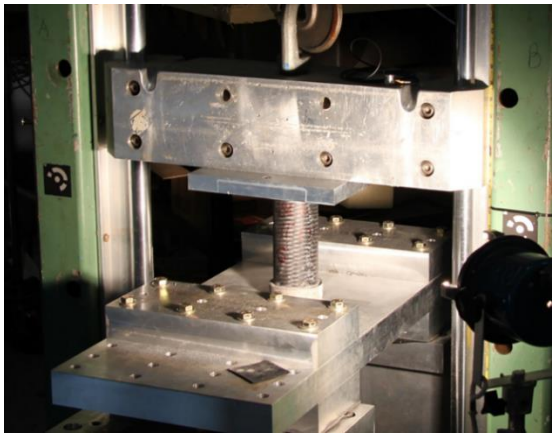

Figure 6. Dynamic crush tube test setup

Tests were conducted on several specimen sample configurations for each material including specimens of varied layup direction, and with internal foam material. The subset of results pertinent to the selection of the material system for use in the EA system development is provided in this report. A more detailed overview of the full test program and results can be found in Littell et. al. 2019 [8]. During initial testing, a ±45° fabric layup was found to produce the most desirable EA response across each material, as quantified by crush consistency and energy absorbing efficiency. The following results are from composite specimens using this layup orientation. During the dynamic impact of the composite tubes, each material system exhibited a different crush response of the tube walls. Images of each tube material during crushing can be seen in Figure 7. The C/C material was found to tear under the dynamic impact, which corresponds to the brittle nature of the carbon fiber. The C/K material produced a uniform folding effect in the walls as it was crushed, with the folding occurring on the top of the tube at the point of impact. The C/U material produced

a folding effect similar to the C/K material though the folds were generally much larger and occurred near the bottom of the tubes rather than the top. Overall, the C/K material produced the most consistent crush

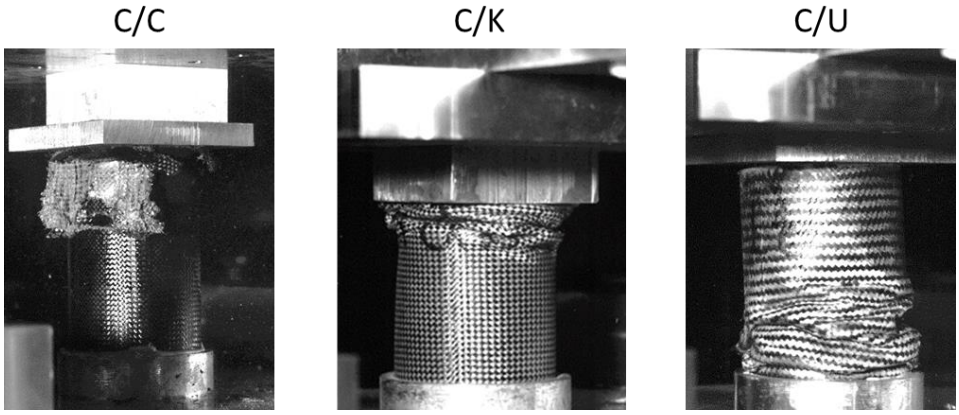

Figure 7. Crush patterns of evaluated composite materials.

response during the impact tests.

Average accelerations measured on the impactor during the tests of each tube material are shown in Table 2. On average, the C/C material produced the highest acceleration and the least amount of crush displacement. This is consistent with the stiffer material properties of the C/C material Both the C/K and C/U materials produced similar average acceleration values, with C/K being slightly lower at 16.9 g compared to the C/U material at 17.9 g. Although the C/U material produced only slightly higher average accelerations than the C/K material it exhibited larger displacement. Compared to C/U material, the C/K material was able to absorb more impact energy, thus reducing acceleration over a shorter crush distance.

Table 2. Dynamic Crush Results

Material	**Average Acceleration (g)**	**Crush Displacement (in)**
C/C	28.2	2.6
C/K	16.9	3.8
C/U	17.9	4.1

Based on the results of the dynamic crush tube testing, the C/K material, with a ±45° layup was selected as the optimal material, of those evaluated, for use in the EA system development. Although both the C/K and C/U exhibited improved ductility over the baseline C/C material, the C/K material produced a more consistent crush response and was more efficient at reducing impact acceleration over a shorter distance. The test results indicated that the C/K material could achieve sustained loading below 20 g through a consistent wall folding mechanism with limited crush initiation force. With an appropriate material selected, the next step was to develop a geometric wall design to increase EA efficiency within the component. To begin the design optimization process a predictive model of the C/K material was needed.

4.3 Material Models

A Mat_58 model of the C/K material was developed in LS-Dyna based on the material parameters generated from the coupon tests conducted. The Mat-58 material model is a continuum damage mechanics model intended to represent composite tape laminates and woven fabrics. Inputs to the material model include stress-strain properties tension, compression, and shear. A stress-limiting damage factor along with maximum strength values and corresponding strain in each direction are also included to predict damage effects within the material. The material parameters defined for the C/K material based on the coupon level test data is provided below in Table 3. Additional details on selection of these parameter values can be found in Jackson et. al [9].

Table 3. Baseline Mat-58 parameters for C/K material

Density, lb-s^2/in^4	1.29E-4
Longitudinal Young's modulus, psi	6.3E+6
Transverse Young's modulus, psi	2.76E+6
Shear Modulus, psi	3.25E+5
Stress limit of nonlinear portion of the shear curve, psi	4.50E+3
Strain limit of nonlinear portion of the shear curve, psi	0.0246
Poisons ratio	0.1095
SLIMT1	0.8
SLIMC1	1.0
SLIMT2	0.8
SLIMC2	1.0
SLIMS	1.0
ERODS	0.5
FS	-1
E11C, in/in	0.007
E11T, in/in	0.0143
E22C, in/in	0.012
E22T, in/in	0.025
GMS, in/in	0.065
XC, psi	4.00E+4
XT, psi	8.90E+4
YX, psi	2.50E+4
YT, psi	5.40E+4
SC, psi	4.70E+3

To verify the effectiveness of the developed material model, a FEM was developed to replicate the conditions of the tensile tests. In this model, the tensile coupon was represented by a shell part with an element mesh length of 0.125 in. Simulation results were found to be consistent at and below this mesh density. Although Mat-58 does not include rate dependency, a rate sensitivity study was performed to ensure tensile pull rate did not affect simulation results. Results were found to be consistent below 100 in/min and thus this rate was used in simulation rather than the tested rate to save computation time. Coupon tensile test simulations were run using LS-Dyna Version R10.1 on 8 processors and had an approximate run time of 5 minutes. Simulation results were compared to the original four ply coupon tests conducted as well as tests on eight ply specimens, performed in the same manner, which were added to ensure properties were consistent across various fabricated layups. Comparison plots showing model predicted stress vs. strain response compared to tested response in each material direction is shown in Figure 8.

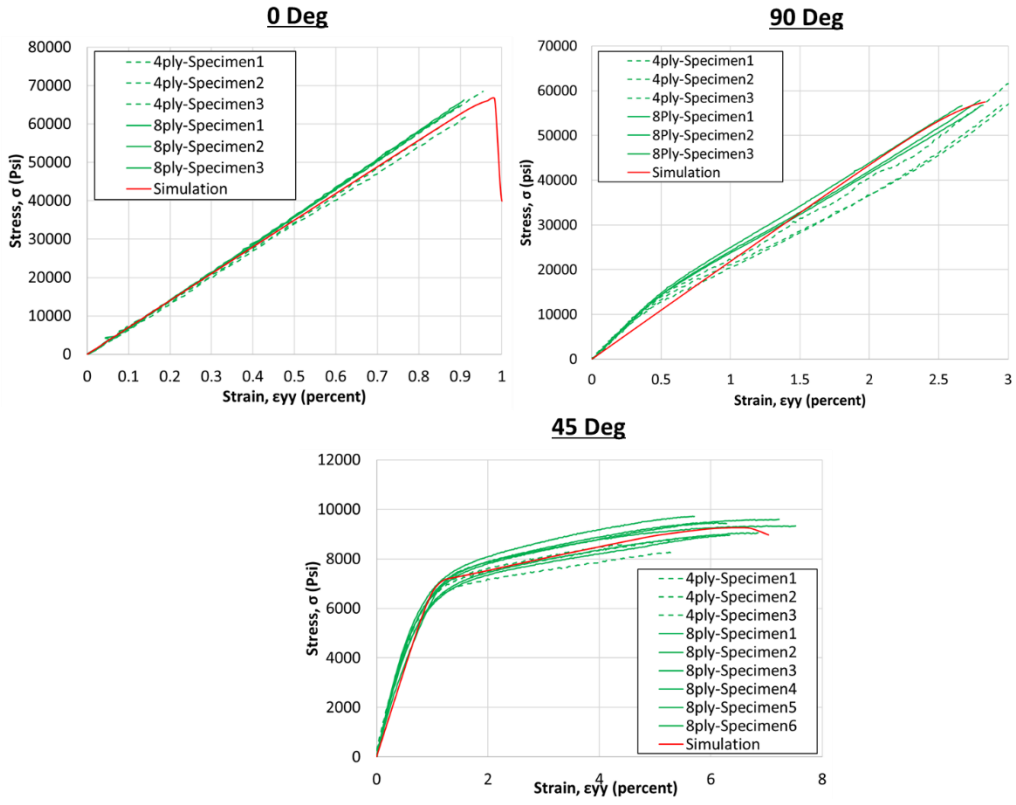

Figure 8. Stress vs. Strain correlation results for baseline C/K material.

The predicted stress-strain response by the developed Mat-58 material model was shown to closely match measured responses in each material direction. The model results were well within test variability both between tests of the same and different ply amounts which showed minimal variation between them. These results provided evidence that the developed material model was effectively predicting material stiffness in

each direction. Next, the flat-walled tube tests were simulated to verify the model's ability to predict material damage, which is vital for accurately determining EA response.

FEMs of the flat walled tubed specimens described in the Section 4.2. Preliminary Component Testing were generated and simulated in the tested conditions in order to evaluate the effectiveness of the generated C/K material model in predicting EA crush response in dynamic loading conditions. The tube model was generated using quadrilateral shell elements matching the dimensions of the tube specimen, with an average mesh length of 0.2 in. The impactor was represented using a rigid solid element block with inertial properties defined to represent its mass. An initial velocity was assigned to the impactor model to replicate the dynamic impact event, and acceleration was measured at its CG for comparison to the test data. A full description of the generated model and subsequent correlation can be found in [8]. A reprinted comparison between measured test and simulation results for the C/K tube impact is shown in Figure 9.

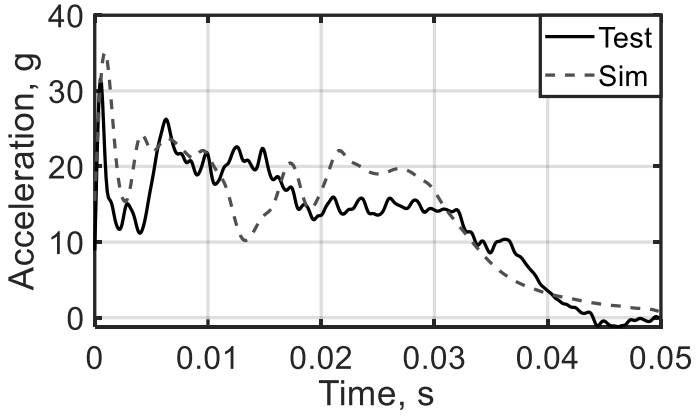

Figure 9. Dynamic correlation results for baseline C/K crush tube.

The developed material model of the C/K material produced close correlation to the measured acceleration elicited during the crush tube impact test. The initial peak acceleration required to initiate tube crushing was closely matched by the simulation along with the average steady state crush acceleration. The timing of each event, crush initiation, steady state crush, and the impactor coming to rest were also closely predicted by the developed model. These results provided confidence in the generated C/K material model for use in predicting EA crush response during further component development efforts.

5 Energy Absorbing Component Development

5.1 Crush Tube Design

5.1.1 Geometric Optimization

The first EA component to be designed using the selected C/K material system was a composite crush tube which could be integrated into seat or landing gear structures to absorb energy during dynamic impact

events. Although the flat walled tube specimens tested during the tube selection process showed adequate EA performance, there was still an opportunity to reduce the crush initiation load, thereby improving EA efficiency. In addition, an analytical evaluation of the flat walled tubes under multi-axis loading conditions showed poor response due to the wall collapsing. Initial analytical investigations into improving crush tube response showed that the addition of curvature into the wall geometry improved crush stability under off-axis loading [8]. To further explore the effects of wall geometry changes on crush response, several crush tube geometry designs were evaluated both analytically and through test to identify a geometry better suited to improve EA efficiency and off-axis stability. The four tube wall geometry designs which were evaluated are shown in Figure 10. The Dimple design was composed of semispherical indentations across the wall. The Accordion design was composed of a sinusoidal curve repeating along the length of the tube wall. The Helix design was composed of a curve progressing down the length of the tube in a helical pattern. The Flower design was composed of eight curved protrusions, parallel and spanning the length of the tube. Each initial design was evaluated analytically to assess the wall geometry most suitable for further EA development.

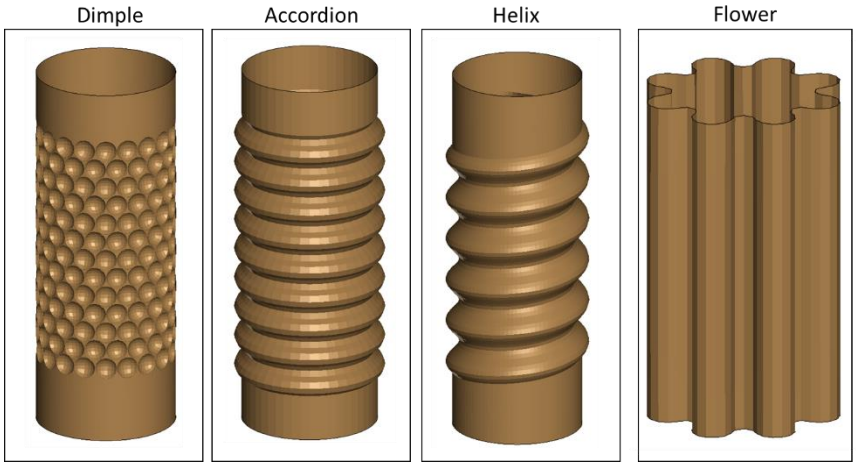

Figure 10. Crush tube design geometries.

The four tube wall designs were simulated in the drop tower test environment model generated for the initial flat wall model verification effort. Each design was modeled using quadrilateral shell elements with a consistent mesh length of approximately 0.2 in. Each tube design was simulated in an impact condition with a 102-lb impactor mass and impact velocity of 20 ft/s. Acceleration time history results for each tube design can be seen in Figure 11.

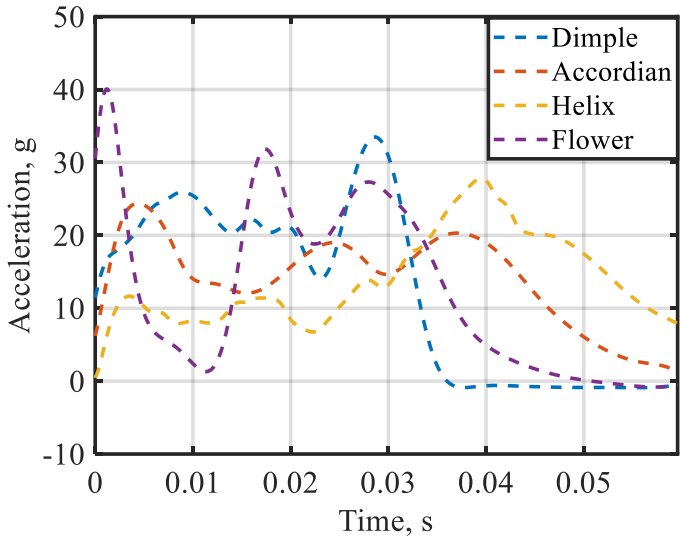

Figure 11. Predicted crush tube design results.

The EA mechanism of the Dimple design aimed to absorb energy through piecewise fracture of the dimple sections within the wall rather than through consistent bending and folding of the material. This produced a reasonably efficient EA response, as the acceleration produced during crush initiation was close to that which occurred during steady state compaction of the tube. However, the remaining energy was not enough to produce fracture in the material and thus was transferred somewhat rigidly through the structure resulting in the large spike in acceleration towards the end of impact. The Accordion design exhibited a very stable EA response produced by folding at the ridges of the wall geometry. This design produced a slightly higher initial crush acceleration than that which occurred during steady state crushing but overall produced the lowest peak acceleration. The Helix design produced a very low crush initiation acceleration but resulted in an asymmetric crush the through the tube wall and a final acceleration on the high end of the evaluated components as the tube compacted fully. The Flower design produced the highest peak acceleration as its design was particularly stiff in the vertical direction and thus required significant energy to initiate crushing. Based on these results, the Accordion design was selected as the geometry which most effectively minimized peak acceleration while exhibiting a stable crush response in the evaluated impact condition.

After selection of the Accordion crush tube design, the next step was to optimize specific aspects of the wall geometry in order to improve EA efficiency. This optimization began by examining the angle of the sinusoidal curvature in the wall. The angle of curvature was varied between 0°, 30°, and 60°, with 0° resulting in the deepest curve and 60° producing the shallowest curve. Tube models with each angle are shown in Figure 12. Each tube curvature was simulated in the same conditions used to evaluate the initial

tube designs. For each condition, acceleration time histories recorded during the simulated impact are shown in Figure 12. The 30° curvature design produced the lowest peak acceleration of the designs evaluated. In addition, it produced a more ideal EA response shape, with acceleration measured at crush initiation closely matching that measured during steady state crushing of the tube. The 60° tube exhibited a higher acceleration required for crush initiation, while the 0° tube required less crush initiation acceleration, but absorbed less energy and thus produced higher peak acceleration as the tube reached full compaction. Based on these results, the 30° angle of curvature was selected as the curve shape for the Accordion design.

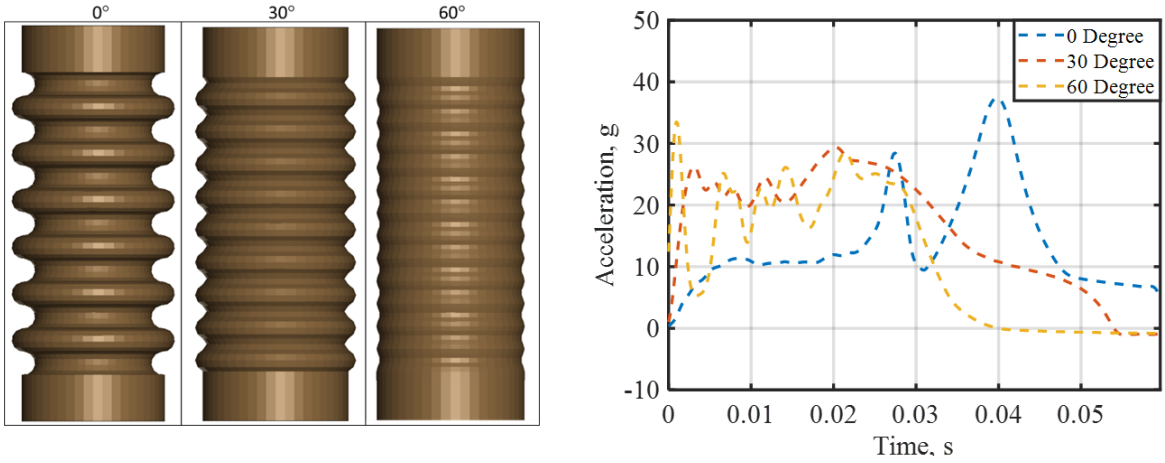

Figure 12. Accordion crush tube wall curvature (left) and effects on impactor acceleration (right).

After down selecting to the Accordion wall geometry with 30° curvature, a verification test was conducted to ensure the developed FEM was accurately representing the physical response of this crush tube design. The tube specimen was tested in the 15-ft drop tower with an impactor mass of 103 lb and an impact velocity of 17 ft/s. The tested conditions were then simulated using the developed Accordion tube FEM. A comparison between impactor acceleration measured during the test and predicted by simulation is shown in Figure 13. In general, the FEM closely predicted the EA response of the tube throughout the impact event. Acceleration predicted at crush initiation closely matched that measured in test. Steady state crush acceleration and peak acceleration measured after tube compaction were both very similar, with predicted peak acceleration being within 10% of that measured in test. The simulation predicted a slight drop-off in acceleration mid-crush which was not observed in the test as well as an ~0.005s delay in the time to peak, however, during the optimization phase these characteristics are not as critical to predict as the initial, peak, and final accelerations. Overall, the correlation between test and simulation provided confidence in using the model to continue to identify design improvements, particularly with regards to metrics such as crush initiation acceleration and peak acceleration measured during impact.

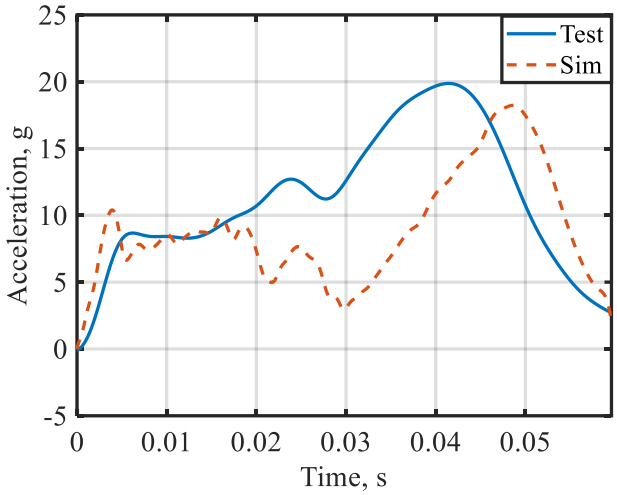

Figure 13. Correlation between test and simulation of Accordion crush tube component impact.

To further improve the EA efficiency of the Accordion crush tube design, an analytical optimization was conducted to define an optimal wall shape, fabric orientation, and wall thickness which would work across a range of relevant occupant masses relevant. This design optimization was conducted using Hypermesh interfaced with LS-Dyna using LS-Opt. Perturbations of the tube curvature were defined using the shape morphing feature within HyperMesh. The tube curvature was bounded at ±30% over the baseline for the optimization analysis. Tube wall thickness was varied between 0.05 in and 0.1 in, through parametrization of the composite part definition within LS-Dyna. Three parallel simulations were conducted for each variable perturbation, and each simulation was conducted similarly to those described in the previous crush tube evaluations. In these simulations, the drop mass was varied in order to evaluate the effects of the design changes on absorbing energy for different occupant masses. The masses used were 100 lb, 170 lb, and 225 lb to approximate the weight of a small female, mid-size male, and large male respectively. The optimization effectiveness was quantified by changes in peak impact mass acceleration measured in each simulation. A full description of the optimization process and results can be found in Putnam et al. 2020 [10]. The optimization process led to the selection of an accordion design with a 20% curvature increase from the baseline and a total wall thickness of 0.062 in, which translated to 5 layers of the 0.0124-in C/K fabric. With the optimized EA tube geometry selected, the next phase of this project was to develop an energy absorbing seat system utilizing this crush tube design.

5.1.2 EA Seat Sub-system Design and Updated Material Model

To evaluate the effectiveness of the developed Accordion crush tubes to improve occupant safety in a relevant environment, a seat design utilizing the tubes to absorb energy along the vertical impact direction was generated. The EA seat design was composed of a generic unibody seat bucket mounted on an aluminum fixture with two guide rails located near the approximate horizontal (front/back) center of the seat pan. EA tubes were fit over the guide rails, between the seat bucket mount and floor attachment

brackets. The guide rails restricted motion of the seat to the purely vertical (up/down) direction and forced any vertical load to go through the seat into the crush tubes, thus absorbing impact energy in this direction. The development of the EA seat design is discussed in further detail within Littell et al. 2025 [11]. Images of the developed EA seat, including a closeup of the crush tubes installed on the seat rail system are reproduced in Figure 14.

Figure 14. EA seat design utilizing Accordion crush tubes: full seat (left) and closeup of crush tubes (right).

During the design of the EA seat system using the Accordion crush tubes, the resin system used in the C/K material fabrication was updated. The WS 105/205 system used in the original crush tube development effort was updated to a higher strength resin system, EPON Resin (Westlake Chemical) 828 with Epikure Curing Agent (Westlake Chemical). This decision was made to increase the relevance of these EA designs to future air mobility vehicles that would require aerospace grade materials throughout all components. The updated C/K material with EPON 828 resin system was characterized through a series of coupon tests in a similar manner as the original WS 105/205 system.

Tensile tests were performed on 10-in. x 1-in. coupon specimens composed of 8-plys of the C/K material fabric with the EPON 828 resin material system cured at room temperature. Specimens were cut at either a 0°, 90°, or 45° orientation along the length to quantify the warp, fill, and shear properties of the material system respectively. Tensile tests were performed at a pull rate of 0.1 in/min until specimen failure. The

properties generated from these tests were input into an updated Mat-58 material model for use in FEM simulation of the material system. The properties generated from the coupon tests are listed in

Table 4.

Table 4. Mat-58 parameters for C/K material with EPON 828 Resin material system

Density, lb-s^2/in^4	1.29E-4
Longitudinal Young's modulus, psi	8.0E+6
Transverse Young's modulus, psi	2.3E+6
Shear Modulus, psi	2.0E+5
Stress limit of nonlinear portion of the shear curve, psi	4.60E+3
Strain limit of nonlinear portion of the shear curve, psi	0.03
Poisons ratio	0.1095
SLIMT1	0.8
SLIMC1	0.8
SLIMT2	0.8
SLIMC2	0.8
SLIMS	0.8
ERODS	0.5
FS	-1
E11C, in/in	0.013
E11T, in/in	0.009
E22C, in/in	0.010
E22T, in/in	0.028
GMS, in/in	0.142
XC, psi	3.30E+4
XT, psi	7.00E+4
YX, psi	2.00E+4
YT, psi	6.00E+4
SC, psi	6.00E+3

To verify the effectiveness of the developed C/K with EPON 828 resin system material model, the FEM previously generated for material model verification was used to compare test to simulation predictions. A comparison of stress strain data computed in both test and simulation for material direction tested is shown in Figure 15. The developed material model was found to closely replicate the stress-strain response of the tested specimen. The only aspect the material model was not able to replicate was a slightly non-linear response shape in the 90° (fill direction) testing. The material model elastic modulus was fit to center the data in this direction. These results gave confidence in using the updated material model to simulate crush tubes fabricated with the EPON 828 resin material system.

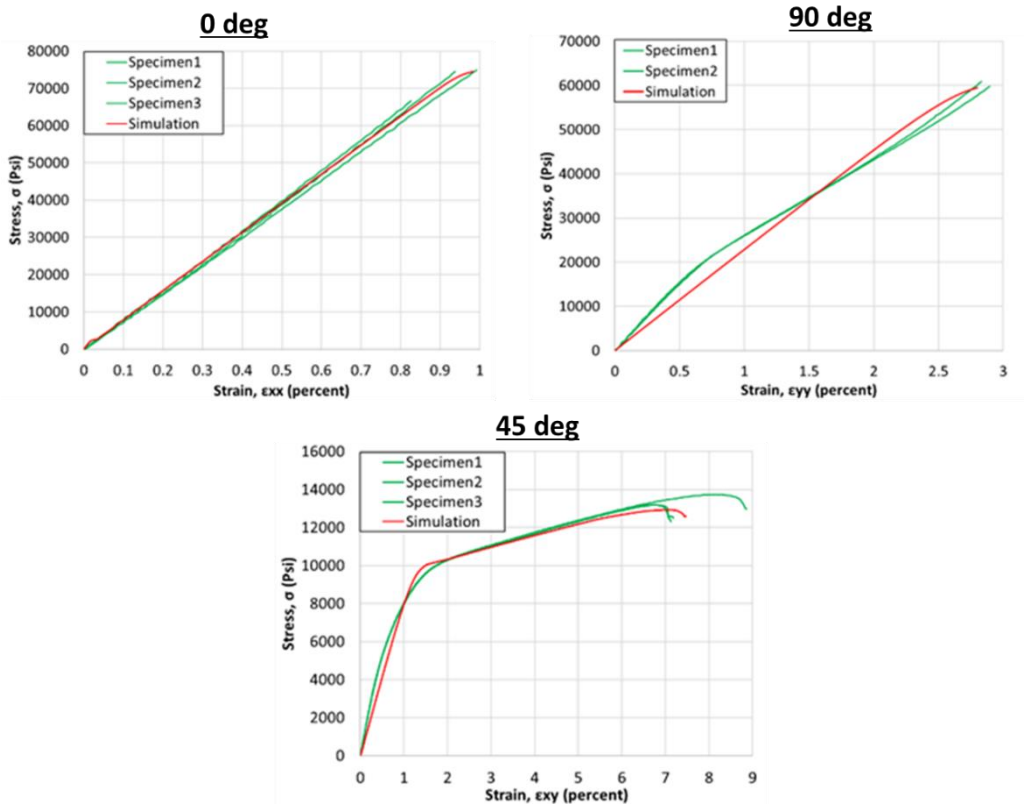

Figure 15. Stress-Strain correlation results for C/K material with EPON 828 resin.

After verifying the updated material model at the coupon level, sample crush tubes were fabricated to the final optimized design, described in Section 5.1.1, with the EPON 828 resin material system. Specimens were fabricated in two lengths, the first was made with the baseline crushable wall length of 6 in while the second used a slightly longer length of 7 in which had showed improved response in preliminary seat sub-system analyses. The longer tube was tested with an impact speed of 15 ft/s while the shorter tube was tested with an impact speed of 20 ft/s. Testing the shorter tube at a higher impact velocity and the longer tube at a lower impact velocity bounded the potential impact response between partial and full compaction of the tubes. A 104-lb. impact mass was used in each test. Each test was simulated using the drop tower environment FEM previously described in Section 4.3 and representative FEMs of each fabricated tube. Simulations were conducted using LS-Dyna version R14.0 single precision. Results showing a comparison

of measured and predicted impactor acceleration in both the 6-in and 7-in tube tests are provided in Figure 16. Results showed the developed FEMs closely predicted the initial, peak, and steady state crush responses in the impactor throughout both test conditions. The model was particularly accurate in predicting the rise in peak acceleration during full compaction in the 6-in tube test as well as the steady state crush followed by a gradual drop-off in acceleration in the 7-in test. These results verified the capability of the generated tube models, with the EPON 828 resin system, to accurately predict EA response over a range of potential loading environments prior to their use in sub-system level analyses.

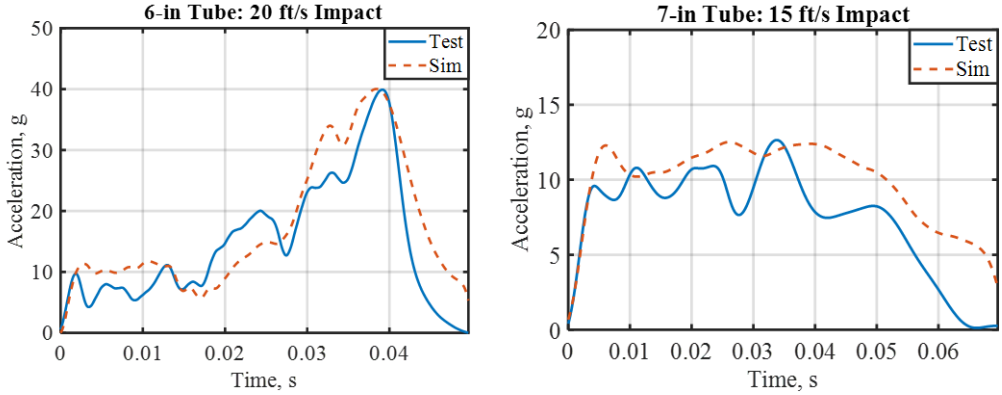

Figure 16. Correlation between test and simulation of Accordion crush tube component impact with C/K material utilizing EPON 828 resin.

5.1.3 Seat Sub-system Verification

To assess the effectiveness of the developed EA seat with the Accordion crush tube design, a series of drop tower tests were completed using the 30-ft drop tower. The EA evaluation tests were performed as part of a much larger seat test series which is described in full detail within Littell et. al. 2025 [11]. To quantify the effectiveness of the developed EA sub-system across various occupant sizes, tests were performed using three different sizes anthropometric test devices (ATDs), the Hybrid III 5th Female, FAA Hybrid III 50th, and Hybrid III 95th (Humanetics). Photos of each ATD size fit into an EA seat within the drop tower are shown in Figure 17. The ATDs were tested in both an EA seat, as described in Section 5.1.2, and a fully rigid seat which was composed of an aluminum frame connecting the floor to the same unibody seat bucket used in the EA seat. Each seat and ATD combination was tested under a 19 g and 31 g impact acceleration pulse, similar in shape to the certification pulses described in FAA regulations 14 CFR § 23.562 [3] and 14 CFR § 27.562 [4], respectively. Compressive force measured in the lumbar spine was used as the primary comparative metric between the seat designs to determine the effectiveness of the EA system in absorbing the impact energy of the test.

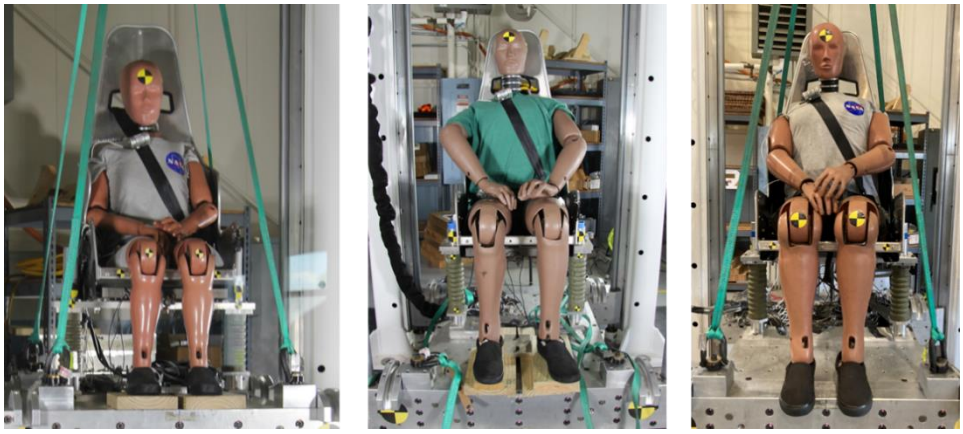

Figure 17. ATD drop tower test setup: Hybrid III 5th (left), 50th (middle), 95th (right)

Comparisons between the compressive lumbar load measured in each ATD on the rigid and EA seats during both the 19-g and 31-g tests are shown in Figure 18. The EA tubes dramatically reduced the peak force applied to the occupant surrogates compared to rigid seat test conditions, particularly when the rigid seat conditions produced greater than 1,000 lb. lumbar force. The FAA 1,500 lb. limit for the Hybrid III 50th ATD was achieved in the 19-g condition with the EA system. In the 31-g EA test the Hybrid III 50th and 95th produced forces just above 1,500 lb. towards the end of impact as the tubes reached full compaction. These results clearly demonstrate that the developed EA tubes reduce spinal injury risk. However, the results also indicate the need for additional EA systems that provide further protection for higher energy impact environments.

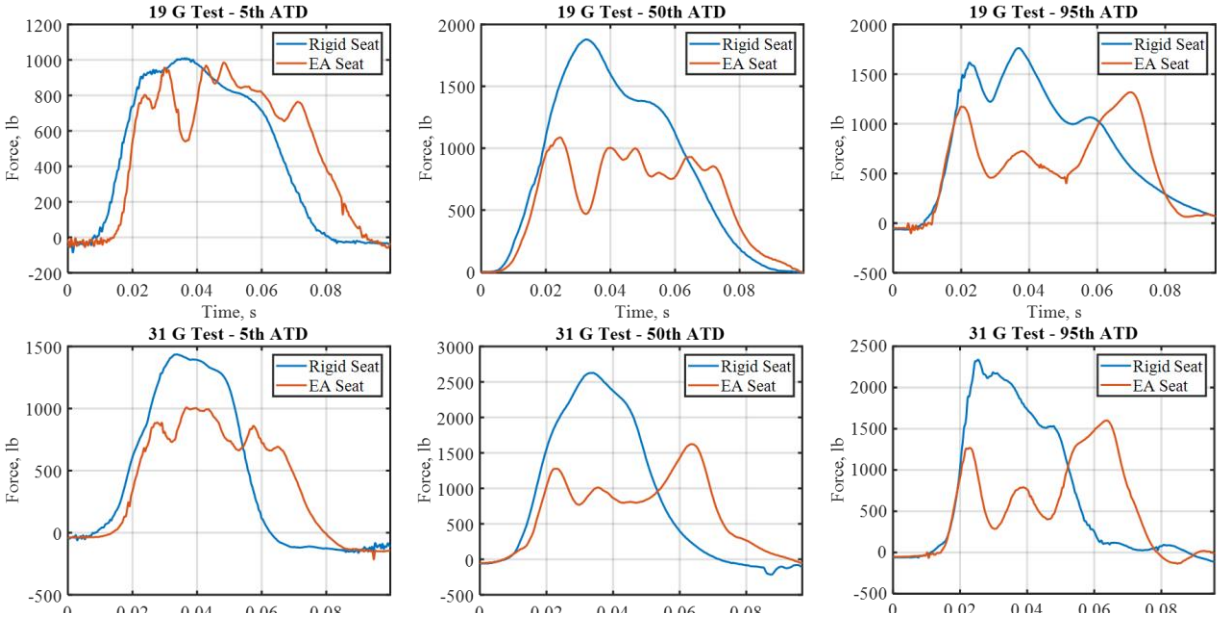

Figure 18. Effect of EA seat on lumbar load response during ATD drop testing.

In addition to the seat level drop tower tests, representative FEMs were generated and simulated within the tested conditions to evaluate the predictive capability of the seat level sub-system FEM. The seat FEM development is described in greater detail in Putnam 2024 [12] and Jones et al. 2025 [13]. Correlations between compressive lumbar force measurements in the EA seat tests and model predictions are shown in Figure 19. The generated FEMs were found to closely predict the compressive lumbar force time histories measured in test, particularly within the 5th and 50th ATD configurations. Peak lumbar force was predicted to within 10% in each of the conditions evaluated. The shape and duration of the lumbar force was closely matched in the 5th and 50th ATD, however, in the 95th ATD FEM the initial force was slightly overpredicted resulting in underpredicting the final force peak measured in test. Overall, these results provided a high level of confidence in using the developed FEMs to predict peak lumbar force for each occupant size and a high level of confidence in predicting the full load time history in the 5th and 50th ATDs.

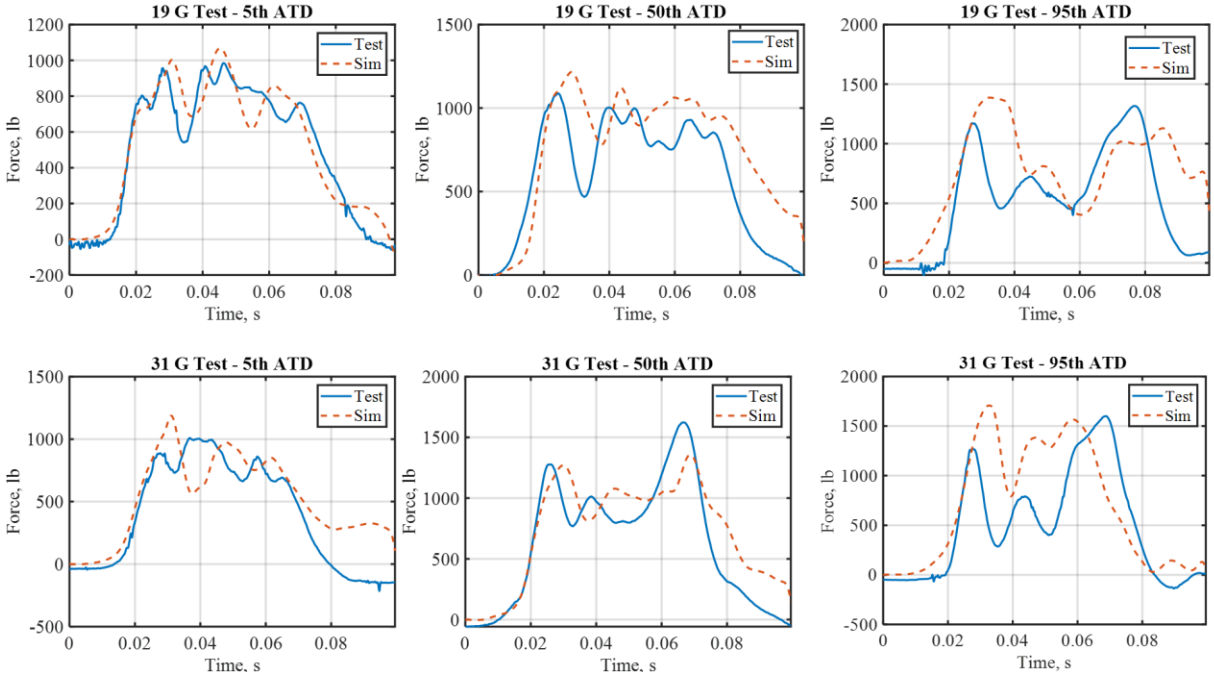

Figure 19. Correlation of simulation to results of ATD drop tests within EA seats.

With the evaluation of the developed Accordion tube design in an EA seat sub-system complete, efforts switched to developing a subfloor EA system which could be used in conjunction with the crush tubes to further improve occupant safety. The design principles and material models developed during the EA tube development were leveraged to design the subfloor EA system.

5.2 Subfloors

5.2.1 Flat Wall Subfloor Assessment

The focus of the EA subfloor design was to generate a self-supporting structure which had robust EA capability across multi-axis loading environments. Previous EA subfloor design work at NASA Langley demonstrated the effectiveness of using wall geometry changes to improve the EA capability of a traditional stringer frame section in a helicopter [1]. Results of this work indicated further improvement in capability under multi-axis loading impacts was possible, but additional horizontal rigidity was needed in the subfloor design. To allow the subfloor component to function independently of the eVTOL airframe structure, a boxed-cruciform geometry was first selected for the EA component. This shape provides rigidity to the subfloor walls, with the goal of maintaining vertical crush capability when any form of horizontal load into the structure is applied. An example of this boxed-cruciform geometry is shown in Figure 20.

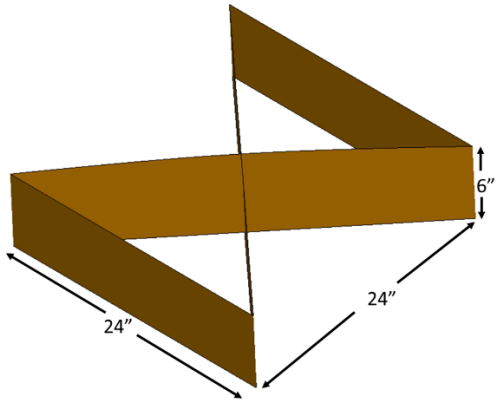

Figure 20. Boxed-cruciform subfloor design.

The boxed-cruciform subfloor design was first evaluated in a flat-walled configuration to define a baseline response for this design geometry. Test specimens of this geometry were fabricated with both the C/C and C/K material. The subfloor specimens were then tested in the 15-ft drop tower. Tests were conducted with a 190 lb. drop mass and an impact velocity of 22 ft/s. Impact acceleration was measured in each test and was used to quantify energy absorbing performance. Acceleration time histories from the C/C and C/K flat-walled boxed-cruciform subfloors are shown in Figure 21. Both specimens produced a large initial peak acceleration of approximately 50 g to initiate the crush in the flat wall geometry design. After the peak value of acceleration occurred, the C/K design shows moderate acceleration during post-peak crushing while the C/C material produced almost no energy absorption after peak acceleration resulting in a large acceleration spike at the end of impact due to the bottoming out of the impactor plate. Similar to the EA tube results, these results confirmed the need for wall geometry optimization to reduce crush initiation force and improve steady state crush response. In addition, these results confirmed the selection of the C/K material in the EA subfloor design.

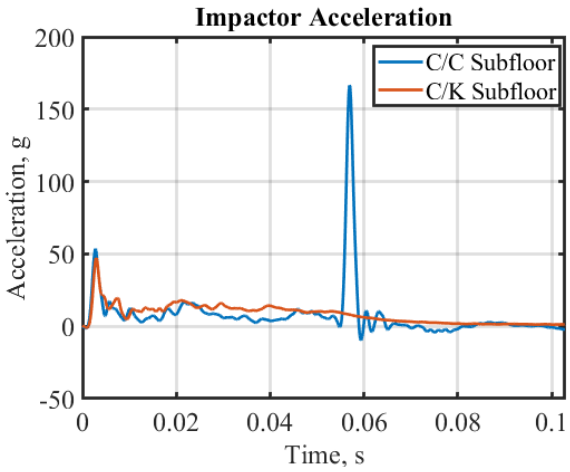

Figure 21. Flat walled boxed-cruciform dynamic crush response with different subfloor wall materials

A model of the flat-walled boxed-cruciform was generated in order to simulate the drop tower tests and confirm the model's capability prior to using it to optimize the wall geometry. The tested geometry was modeled using 0.1-in quadrilateral shell elements. The composite material system was defined within the model in the same manner as the crush tube simulations utilizing the *Mat_58 material card in LS-Dyna. The drop tower environment model developed for the crush tube component test simulation was used to simulate the subfloor tests conducted. The C/K subfloor test was the focus of the correlation as this material system would be used in subsequent design optimization, and a comparison between test and simulation results is shown in Figure 22. The simulation demonstrated close prediction of the peak acceleration observed during crush initiation and the low steady state crush response. In addition, comparison of test and model crush response during and after the test showed a similar folding pattern of the subfloor walls during impact. These results provided confidence in using the composite model to optimize the subfloor design for reduced force required for crush initiation and a more stable wall folding response during crush.

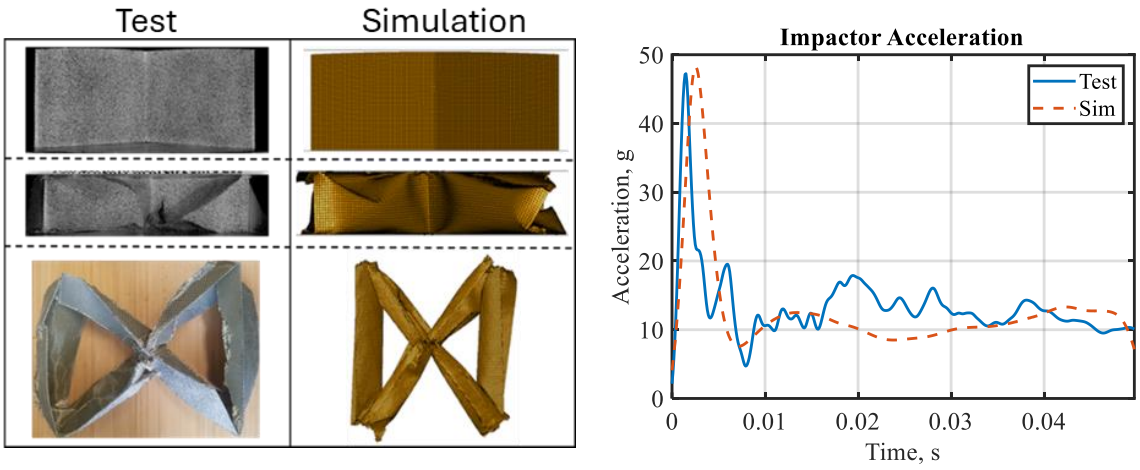

Figure 22. Flat walled boxed-cruciform dynamic crush response and model correlation.

5.2.2 Subfloor Geometry Optimization

In the optimization of the boxed-cruciform subfloor three different wall geometries were considered. First, the flat-walled design was included as the baseline configuration (Figure 23-a). The next design was made up of corrugated walls (Figure 23-b) that matched the curvature of the accordion shape previously optimized for EA crush tube design. This design was named the single accordion (SA) subfloor. The final wall design was composed of two accordion sheets arranged side by side into trapezoidal sections (Figure 23-c). The trapezoidal sections provide a fillable void in which foam could be added to the structure for a high energy impact use case. This design was named the double accordion (DA) subfloor. There were three main criteria on which the subfloors were judged: whether the design was self-supporting, the efficiency of energy absorption, and its robustness to multi-axis loading. To quantify the effectiveness of these designs for meeting the design criterion, a component and vehicle integrated analysis study was conducted. This complete study is described in Putnam et al. 2022 [14] and will be summarized in this section of the current report.

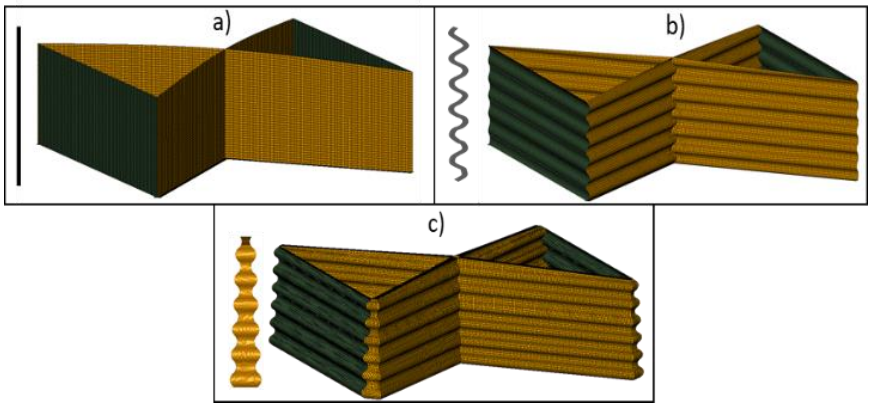

Figure 23. Boxed-cruciform wall geometries: a) flat walled, b) single accordion, c) double accordion.

The three subfloor wall geometries were first evaluated at the component level through simulation of a flat mass impacting the subfloors at varied masses, impact speeds, and impact angles. A schematic of the component level simulation reprinted from Putnam et al. 2022 [14] is shown in Figure 24. Each subfloor design was modeled using 0.1-in quadrilateral shell elements and the previously developed C/K material model to define the material. Each design was initially simulated with four layers of the C/K material oriented in the ±45 orientation. Three and five ply configurations were also simulated to determine the sensitivity of the design to material layup.

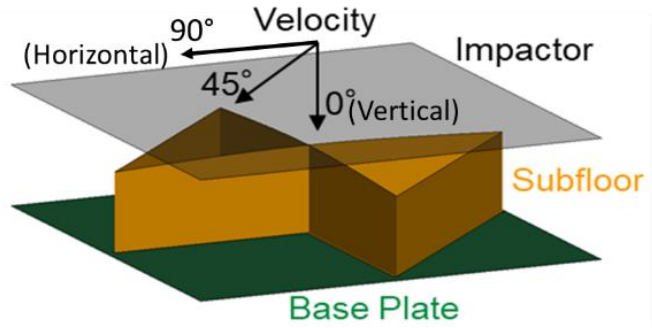

Figure 24. Component level subfloor simulation setup.

Each subfloor design demonstrated the desired response to combined impact loading across the conditions evaluated, producing similar or improved acceleration response time histories in the 0° (vertical) impact and multi-axis loading conditions. An example of this is shown in Figure 25 which compares impactor acceleration during the 0° and 45° impact velocity cases across each subfloor design. In each case, the 45° impact velocity resulted in similar acceleration time history shape indicating no change in crush mechanism with multi-axis loading condition. Peak acceleration was decreased in the 45° velocity conditions as the

total impact energy was kept constant across impact angles resulting in reduced vertical impact velocity in the 45° case compared to the 0° case. The robustness of the responses to impact angle indicated the capability of the overarching box-cruciform design shape to maintain wall stability under multi-axis loading regardless of wall design. The flat-walled design produced a poor EA response across the conditions tested, with high crush initiation force and minimal energy absorption afterward. The corrugated walls of the SA design were shown to significantly reduce crush initiation force and improve steady state crush. With the same ply layup, the DA design produced a higher crush initiation acceleration compared to the SA design due to having double the wall material, though its EA efficiency was ideal as the crush initiation closely matched the steady state crush response. The DA subfloor did not produce an identifiable steady state crush response in the 45° velocity condition as the vertical impact velocity was reduced before a steady state crush could be achieved

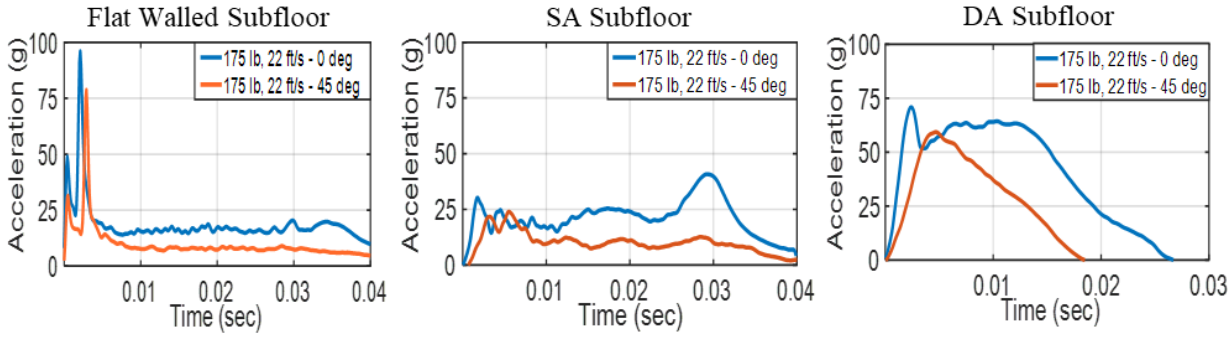

Figure 25. Predicted component level subfloor response to dynamic impact: flat walled (left), SA (middle), and DA (right) designs.

Across the conditions simulated, the flat wall design exhibited poor EA performance, with minimal potential for improvement through changing the composite layup. In the SA design the crush initiation force and energy remaining at full compaction were sensitive to the composite layup, which indicated potential to optimize this design for near ideal energy absorption response depending on the specific environment it is to be used. The DA design similarly was found to be easily tunable using the composite layup in order to produce near ideal EA response in the conditions evaluated.

After evaluating the subfloor designs at the component level, they were integrated into a representative eVTOL FEM [15,16] and simulated in a full-scale crash impact environment to evaluate their performance as standalone EA subfloors within a vehicle structure. A schematic showing the SA subfloor integrated into the vehicle FEM is reprinted from Putnam et al. 2022 [14] in Figure 26. Seats with representative occupant masses were placed over each subfloor and accelerations at the occupant center of gravity (CG) were measured for evaluation of EA effectiveness. The vehicle FEM was simulated in two impact conditions. The first was a vertical impact of 26 ft/s while the second was a combined 26 ft/s vertical and 42 ft/s horizontal impact. Each impact was onto a rigid concrete surface. This 26 ft/s vertical impact condition was selected based on estimated vehicle vertical velocity during a 30 ft/s crash after landing gear has absorbed a portion of the impact energy.

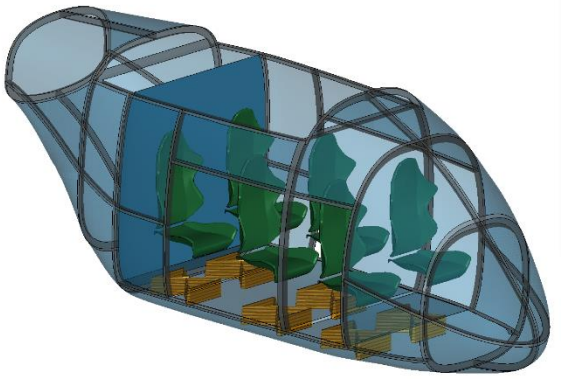

Figure 26. Representative eVTOL vehicle FEM with integrated EA subfloor models.

Acceleration time histories predicted in the middle starboard seat over both impact conditions for each subfloor design are reprinted from Putnam et al. 2022 [14] in Figure 27. Each produced similar acceleration responses in both the vertical and multi-axis loading conditions verifying the directional robustness identified in the component analysis. Both the SA and DA subfloors produced similar acceleration responses with peak accelerations of approximately 60 g measured in the seat. These results were a large improvement over the baseline design which produced seat level acceleration of over 100 g. Based on the results of the component and full-scale subfloor evaluation, the SA subfloor was selected as it significantly improved energy absorption over the baseline design. The tunability and multi-directional effectiveness of the SA design were also important features. While the DA design exhibited similar features and slightly improved peak accelerations in certain conditions, the SA design was ultimately chosen due to ease of manufacturability relative to minimal loss in performance compared to the DA design.

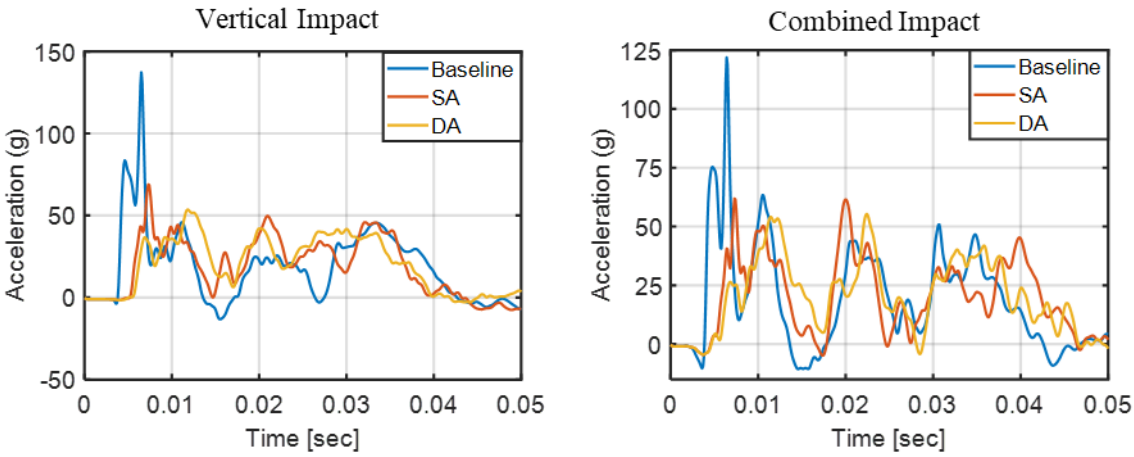

Figure 27. Comparison of seat acceleration response over different subfloor designs within full vehicle impact simulation.

5.2.3 Subfloor Component Verification

After the selection of the SA subfloor design, component level testing was conducted to verify the performance of the SA subfloor. Four component specimens of the SA subfloor, composed of four layers of the C/K composite material, were fabricated for testing. During initial fabrication, weight variations were identified in the specimens and associated with different vacuum application methods during the fabrication process leading to different levels of resin absorption between specimens. The observed differences in the fabrication efforts led to the decision to fabricate multiple specimens in the same configuration to quantify the effect of specimen variability on EA response. The four test articles fabricated were as follows: two specimens with a 45° layup weighing 1.4 lb each, one with a 45° layup weighing 1.7 lb, and one with a +/-45° layup weighing 1.7 lb. Each specimen was constructed of 4 layers of C/K composite. The two specimens with the 45° layup and 1.4 lb weight were tested to identify variability within specimens of equal weight. The 1.7-lb specimen was tested to evaluate the effect of increased resin within the component structure, and the +/-45° layup was tested to identify the effect of fabric orientation on EA response. Each component was tested within the 15-ft drop tower with a 190-lb impact mass and an impact velocity of 22 ft/s. Simulations of the box-cruciform accordion subfloor design were conducted to match each component drop tower test. Differences in specimen weight were accounted for in the model by adjusting the intralayer thickness of the composite, since the specimens with higher weight had increased total wall thickness. A comparison between impactor acceleration measured in test and simulation for each unique subfloor configuration is shown in Figure 28. In the tests conducted, weight variability was found to be the greatest contributor to differences in subfloor response. This is shown by the clear difference between the 1.4-lb subfloors and the 1.7-lb subfloor, with the 1.7-lb subfloor exhibiting a much larger initial peak acceleration during the initiation of the subfloor crushing. This increase in crush initiation acceleration was associated to the increased resin creating stiffer walls, requiring an increased acceleration from the drop mass to begin crush. The +/-45° layup showed slightly higher peak acceleration then the +45° layup configuration, this is

associated with increased wall stiffness in the +/-45° layup configuration. The repeated 1.4 lb +45° test showed similar trends in response but there was variability of approximately 3 g in crush initiation acceleration and differences in acceleration shape during crushing of the two specimens. Simulation results matched the trends observed in the physical testing.

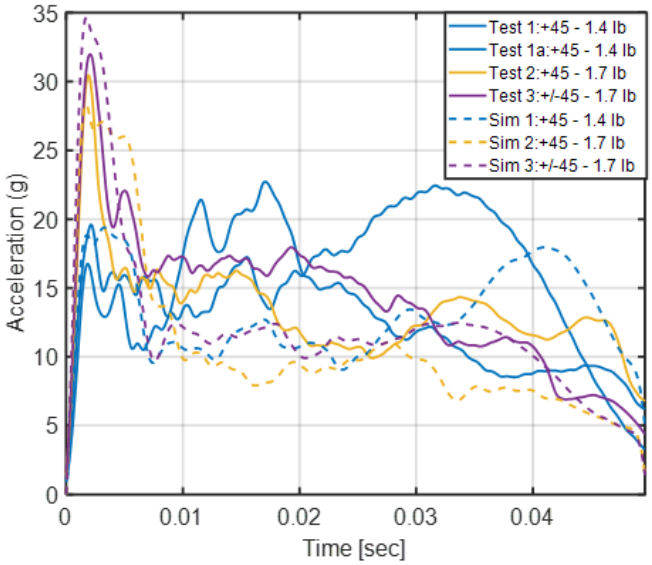

Figure 28. Simulation correlation of impact acceleration to vertical drop tower tests of SA subfloor specimens.

The simulation predicted the increase in peak crush initiation acceleration with increased specimen weight and the change associated with ply layup orientation. In addition, the simulation predicted peak acceleration for each specimen as well steady state response within the range of variability that was observed between the repeat test specimens. These results added to confidence in using the developed FE models to predict subfloor response effects due to changes in composite layup orientation and variations in material density. Based on the results of test and simulation the subfloor fabrication method producing the 1.4-lb. subfloor and a +45° ply orientation was selected for the SA subfloor design.

6 Energy Absorbing System Verification

Following the selection and characterization of the accordion crush tube and SA subfloor designs utilizing the C/K composite material, a full-scale vehicle crash test campaign was undertaken which allowed these EA components to be evaluated within a fully integrated vehicle system. For this test campaign, the developed EA components were integrated into a representative eVTOL fuselage structure developed by NASA dubbed the Lift + Cruise (LC) vehicle design [17,18]. In this test article design, the full vehicle was simplified to capture the cabin structure, replacing components such as the tail, wings, and flight systems with mounted mass. A picture of the LC airframe test article design is shown in Figure 29. A complete description of the test article design can be found in Littell et al. 2023 [18]. The setup, results, and findings

from each test pertaining to the EA components, as well as updates made to the designs based on this testing, will be described in the following sections.

Figure 29. LC airframe test article.

6.1 Full-Scale Vehicle Assessment

To integrate the accordion crush tube design into the LC airframe architecture, an EA seat design was developed similar to the seat system described in section 5.1.2 Seat Sub-System Verification. Two accordion crush tubes were integrated into the seat legs such that as the occupant mass loaded the seat vertically, a plunger in the seat legs would crush the tubes and absorb the impact energy. A picture of the EA seat design used in the LC testing is shown in Figure 30-left. The main difference in seat design between the drop tower tests and the LC test was that for the LC testing, the seat legs were oriented with a 15° tilt from the vertical in order to account for the combined vertical and horizontal loading from the full-scale test environment. The SA subfloor component was integrated into the LC test article along the floor skin (Figure 30-right). The floor skin of the LC test article was designed without reinforcing structure to avoid interference with the response of the added SA subfloors. One SA subfloor was placed under each of the six seats within the test article, two additional SA subfloors were installed in the floor section which held the data acquisition system during testing, and one SA subfloor was installed in the front floor section to provide support during test article build up. Flanges were added to the top and bottom of the SA walls in order to bond them to both the bottom skin of the test article and to the floor sections which were installed on top.

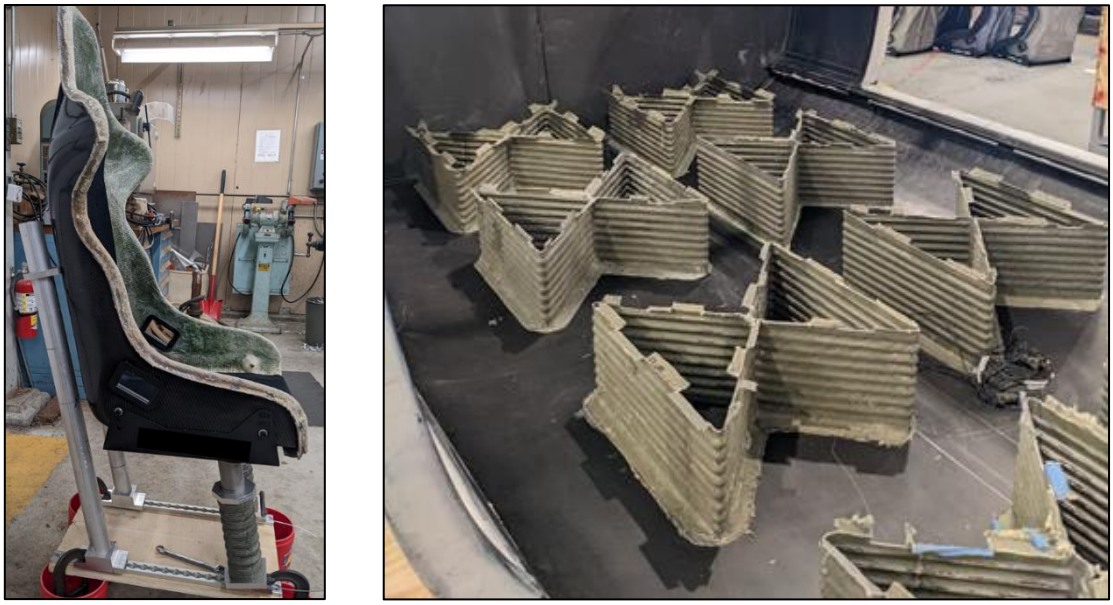

Figure 30. EA components installed in LC test article: seat (left) and subfloors (right).

Six seated ATD experiments were included within the LC test, a full description of these experiments can be found in Littell et al 2023 [18]. This section of the current report will focus on the ATD experiments in the middle row of seats within the LC test article as they provided the most pertinent data with respect to EA component effectiveness. The middle seat row consisted of two Hybrid III FAA 50th ATDs. The ATD seated on the starboard side was in a composite seat pan with rigid seat frame. The ATD seated in the port side was in a composite seat pan with the EA crush tube seat frame. Both ATDs were placed in an upright orientation and were held in the seat using a three-point belt.

The LC test was conducted using the gantry test structure at the NASA Langley LandIR facility. The test was conducted by swinging the LC test article onto a concrete impact surface to induce combined horizontal and vertical impact loads. The impact conditions of the test were 38.1 ft/s horizontal velocity and 31.0 ft/s vertical velocity with a 0.6° nose down pitch and a 2° portside yaw. Snapshots from the test showing the middle row ATDs during the impact event is reprinted from Littell et al. 2023 [18] in Figure 31. The first image shows both ATDs just prior to the structure impacting the ground. At the 0.017 s mark, the EA crush tube begins to stroke while the ATD seated in the rigid framed seat starts to compress downward into the seat. At 0.056 s after impact, the accordion crush tubes of the EA seat have fully stroked while the ATD remained upright, whereas the ATD in the rigid seat began rotating forward as the loading through its spine progressed. No deformation of the rigid seat frame was observed. During this test, the EA seat system behaved as expected and the combined horizontal-vertical loading environment was not found to reduce the effectiveness of the accordion crush tubes during the test.

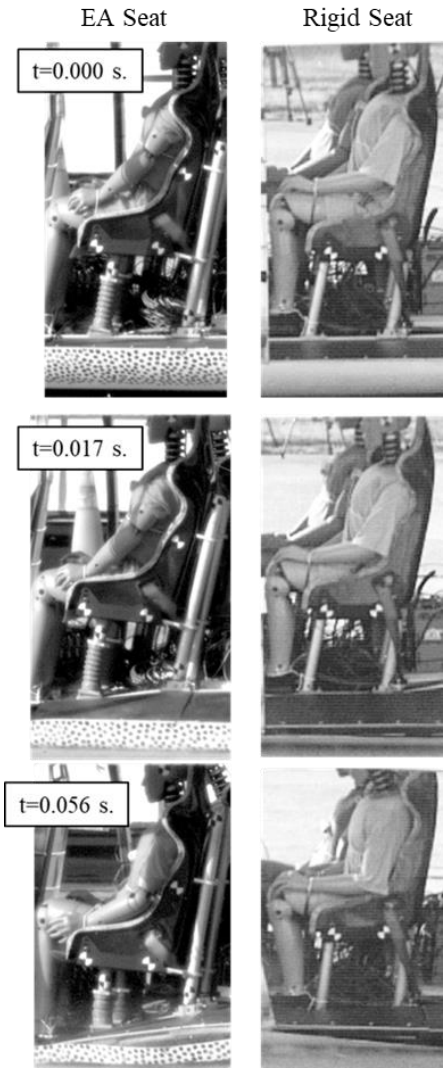

Figure 31. Timelapse comparison of ATDs in EA and rigid seat during LC test.

To evaluate the effectiveness of the EA systems, the lumbar load response was recorded and compared between the ATDs used in the test. A comparison of lumbar load time history between the middle row ATDs is shown in Figure 32. The peak lumbar load in the ATD over the rigid seat frame was 2,500 lb. while peak lumbar load in the ATD within the EA seat was 1,350 lb. These results demonstrated a clear reduction of lumbar loads through the use of the accordion crush tubes in the occupant load path. The engagement of the crush tubes can be seen within the lumbar load time history, with force initially peaking at 1,350 lb. at approximately 0.017 s after which it drops as the tubes begin to compress and eventually levels off to a steady state crush force of approximately 1,000 lb.

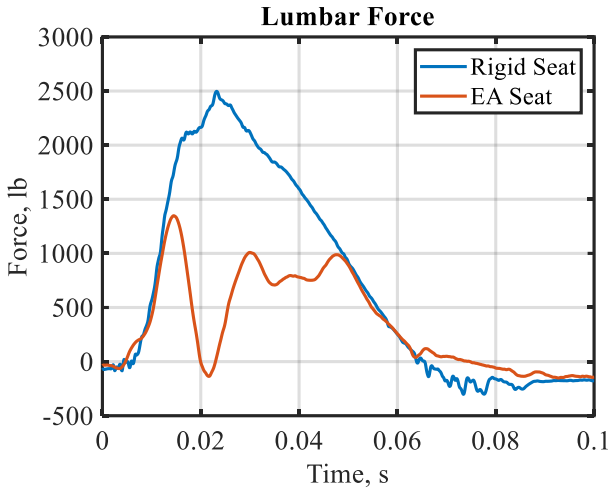

Figure 32. Comparison of measured lumbar force in rigid and EA seats during the LC test.

The SA subfloors were found to be robust to the combined horizontal-vertical impact environment of the test. All subfloors remained intact, and no wall collapse was identified post-test. There was no direct comparison between rigid and EA subfloors as there was for the EA crush tube comparison, however, some effects could be observed on the subfloors from occupant loading. The conclusions drawn from these observations are limited due to an unexpected result of the interaction between subfloor and seat EA response. During the post-test inspections, minimal stroke of the subfloor under the EA seat was observed, while the subfloor under the rigid seat frame was found to have fully stroked. This effect can be seen in the floor acceleration time histories measured under each seat (Figure 33). The peak acceleration at the floor under the EA seat was much higher than that in the rigid seat. This high peak can be attributed to the combined effect of the EA seat on the subfloor crush effectiveness. These results indicated that the accordion crush tube EAs initiated at a lower force than the subfloors, which resulted in the seat EA limiting the impact force to a level below that required to crush the subfloor and thus no impact energy was attenuated at the floor level. Although the seat EA managed to successfully reduce occupant injury risk, these results indicated poor synergy between the two EA components. To improve the combined performance of the two EA components an additional design optimization was conducted.

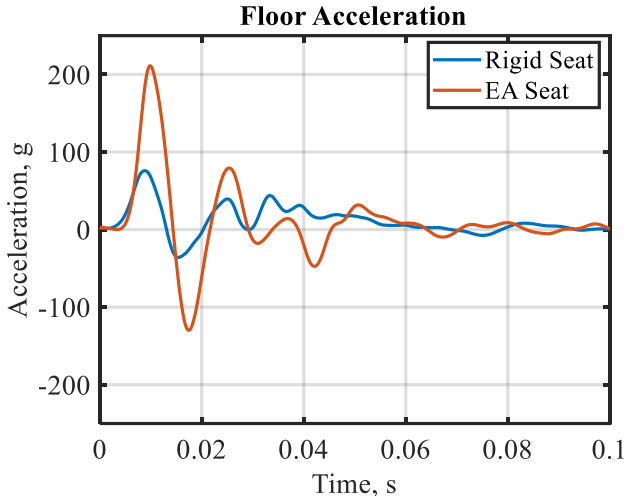

Figure 33. Comparison of floor acceleration measured under the rigid and EA seats during the LC test.

6.2 Energy Absorbing System Optimization

Results from the full-scale vehicle assessment of the combined EA subfloor and seat system indicated that though the accordion crush tubes within the seat were effective at reducing occupant injury risk, the two systems did not work in a cohesive manner. The subfloor essentially required too high of a crush initiation force to work effectively in combination with the EA crush tube design. To overcome this limitation, the subfloor geometry was re-worked with the intention of reducing the crush initiation force while maintaining structural rigidity and EA capacity. After reviewing the SA design, it was concluded that the four wall intersection at the center of the cruciform was producing a stiffness concentration which increased peak force required to crush the subfloor without greatly contributing to the energy being absorbed during steady state crushing. To remove the stiffness concentration, a curved “infinity” shape was selected to replace the boxed-cruciform shape of the original subfloor design. A comparison between the two subfloor shapes can be seen in Figure 34. The infinity shape approximated a figure-8 without the line crossing in the middle, thus removing the intersecting walls. The inward curvature of the infinity shape provided stability to horizontal loads while not overly stiffening the structure at any one location. By removing sharp intersections, the manufacturability of the subfloor design was also improved.

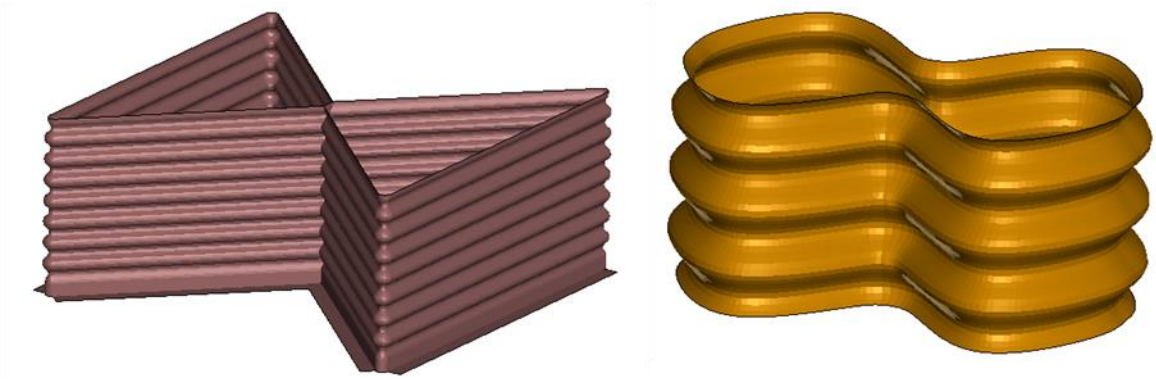

Figure 34. Schematic of SA subfloor design (left) and updated “infinity” subfloor design (right).

In addition to updating the shape of the subfloor design, the wall geometry was adjusted to better match the folding characteristics observed within the accordion crush tube. In the original SA design, the sine function used to define the curvature of the crush tube was also used along the wall length of the subfloor. In the updated subfloor design, the period of the sine curve was scaled by the relative difference in total length between the crush tube and subfloor. This resulted in a similar wall length to curvature ratio which was hypothesized to produce a more consistent wall folding response between the two designs.

To compare the response of the updated infinity subfloor design to the SA design, the infinity subfloor was modeled and simulated in the standard drop tower configuration previously tested with the SA design. The simulated test condition consisted of a 175-lb drop mass, approximating a mid-size male occupant, impacting the subfloor with a speed of 22 ft/s. A comparison of the crushed state of both subfloor designs and impactor acceleration time histories is shown in Figure 35. The SA design has generally shown a sharp acceleration spike during crush initiation followed by a steady state crush acceleration of approximately 15 g in this condition. The infinity design showed significant reduction in crush initiation acceleration with a slightly higher steady state crush acceleration. The infinity design also showed a much more stable crush response with folding in line with the wall corrugation and no significant material tearing. In addition to the more stable crush response observed in simulation, the updated design was expected to improve manufacturability by removing the sharp internal edges. As discussed in section 5.2.3 Subfloor Component Verification, the SA design response was found to be sensitive to resin infusion levels during manufacturing and thus improved manufacturability in the infinity subfloor design was hypothesized to also improve component response consistency.

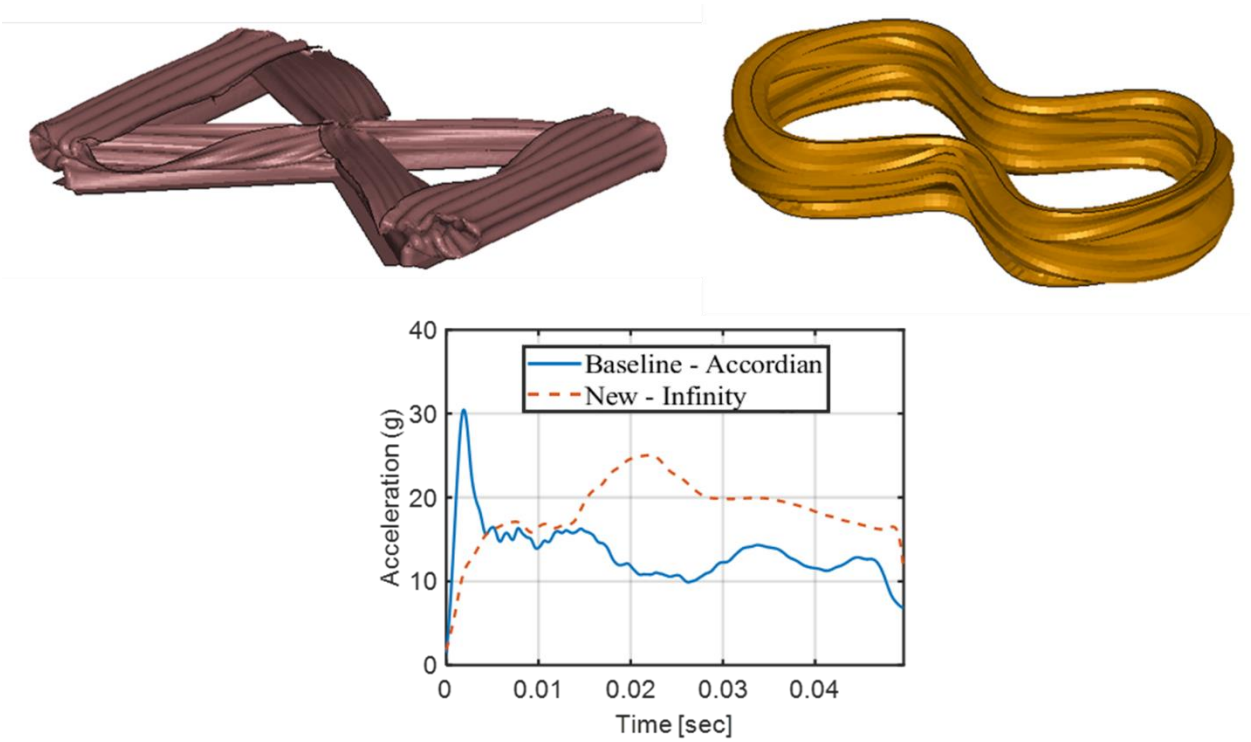

Figure 35. Comparison of crush response and applied acceleration between SA and "infinity" subfloor designs during vertical impact.

To quantify the capability of the infinity subfloor to absorb impact energy in multi-axis loading environments, the subfloor design was evaluated analytically in combined vertical-horizontal (Y) and vertical-lateral (X) loading conditions. In this evaluation, 45° impact velocity conditions were simulated in each direction, with equal total energy to the pure vertical 21-ft/s impact condition previously simulated with this subfloor design. A 175-lb impactor mass, approximating a mid-size male occupant, was simulated in each condition. A schematic of the two impact directions, with respect to the orientation of the subfloor is shown in Figure 36. The infinity subfloor model produced lower impactor acceleration than what was produced in the vertical only impact condition and produced similar acceleration shape. The lower peak values were produced by the reduced vertical component of the velocity vector in the 45° impact conditions. Similar acceleration shape indicates similar crushing mechanics across these impact conditions. Lack of acceleration spiking, low overall accelerative loading, and similar crushing mechanics indicated that the infinity subfloor design effectively absorbed impact energy in combined loading environments. Both the vertical-horizontal and vertical-lateral impact conditions produced nearly matching acceleration curves, which indicate a symmetric crush response to each multi-axis loading direction within this design.

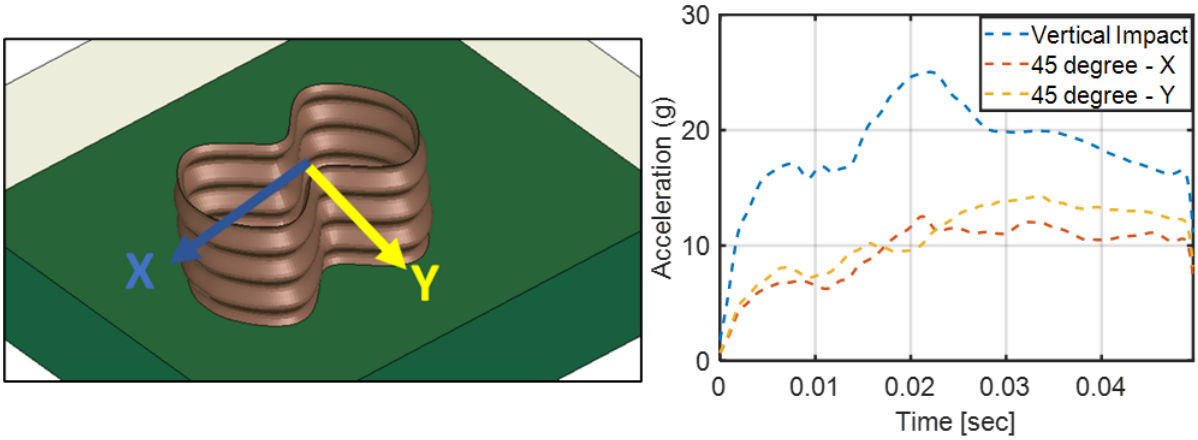

Figure 36. Subfloor multi-axis loading orientations (left) and impactor acceleration results (right).

A combined EA subsystem model, which included the infinity subfloor and seat-level EA crush tube designs, was generated in order to evaluate and optimize the combined effectiveness of the two components to reduce occupant injury risk. The infinity subfloor model was stacked under a generic aluminum seat design with two accordion crush tubes. A rigid plate model was set between subfloor and seat, representing the floor element between components. A rigid plate model was also fixed to the bottom of the subfloor to represent the impacting vehicle surface or the impacting plate used in drop tower testing. An initial impact velocity of 26 ft/s was applied to the bottom plate to represent the vehicle impact environment. A Hybrid III 50th ATD model was fit into the aluminum seat with a 3-point belt to evaluate occupant loads within the model. The combined EA system model, pre- and post-impact simulation is shown in Figure 37.

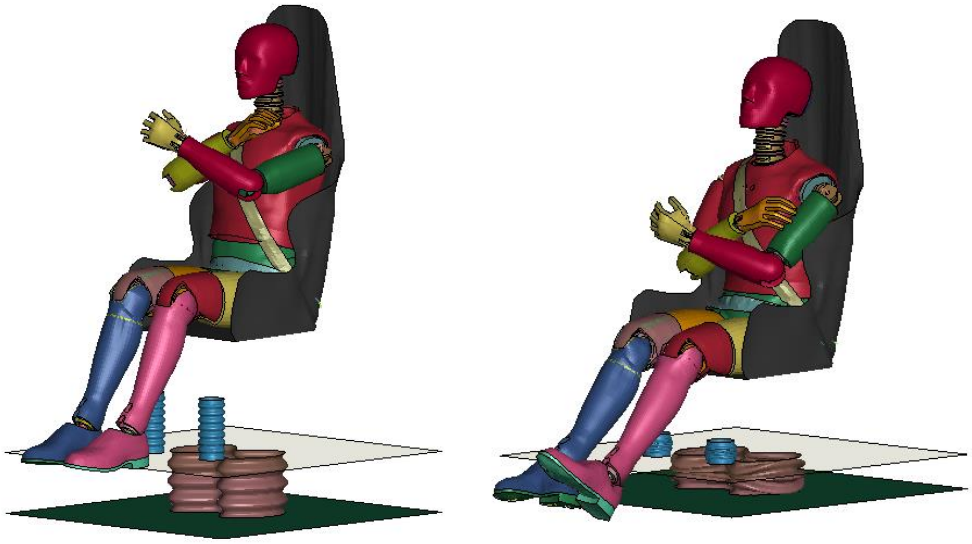

Figure 37. Combined EA subsystem model with Hybrid III 50th ATD.

The baseline simulation of the combined EA subfloor and seat crush tube model predicted both EA components to begin crushing near simultaneously as the ATD lumbar load approached 1,500 lb. This was to be expected as both components had been optimized independently using the 1,500 lb. lumbar load limit threshold. To improve the EA capability of the combined system, the subfloor design was adjusted by reducing the number of fabric layers in the subfloor wall from five to four which reduced the crush initiation threshold for this component. Reduction of the crush initiation force in the subfloor resulted in a differentiation of the subfloor and crush tube activation thresholds. A comparison of predicted lumbar load time history with the baseline and updated combined EA system models is shown in Figure 38. The lower crush initiation point in the updated subfloor can be observed in the reduction in the first lumbar load peak at approximately 0.01 s. The separation of component activation can be identified by the longer delay between first and second peak load and the resulting reduction in the second peak within the updated model.

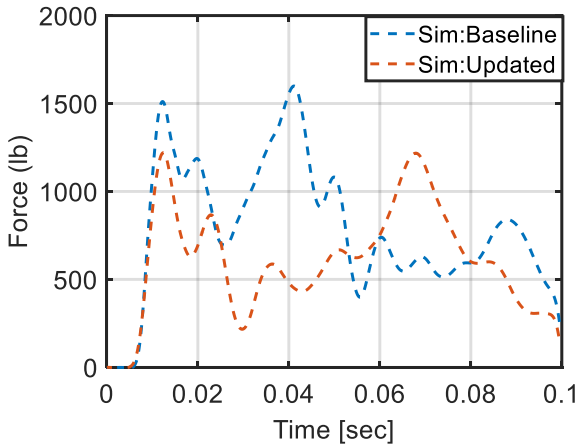

Figure 38. Lumbar load time histories predicted using the baseline and updated EA system models.

After completing initial evaluations of the infinity subfloor design through simulation, component tests were conducted to confirm the subfloor's response under vertical loading conditions. For the tests, a 185-lb impactor was dropped onto the infinity subfloor with an impact speed of 21 ft/s. This test was also simulated to verify the predictive capability of the developed infinity subfloor model. A comparison between the test and simulation mid crush is shown in Figure 39. The simulated model closely predicted the crush response of the EA subfloor throughout the impact event, including prediction of wall folding and tearing mechanics.

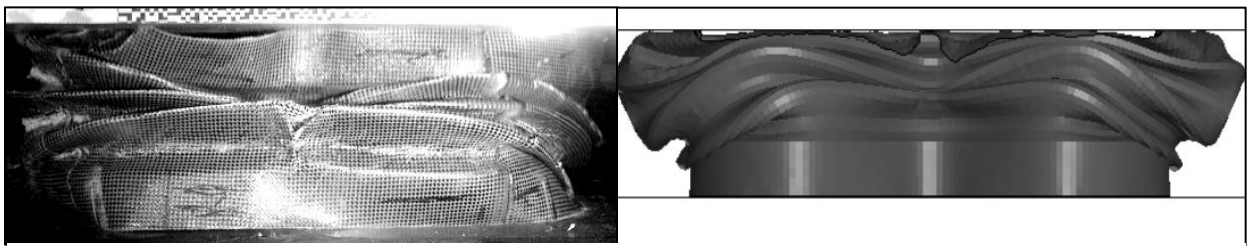

Figure 39. Comparison of" infinity" subfloor crush response observed in test (left) and predicted by simulation (right).

The measured acceleration time history of the impactor during the infinity subfloor test along with that predicted by simulation is shown in Figure 40. The tested subfloor produced an effective EA response with similar acceleration measured at crush initiation and steady state crush of approximately 12 g. At near full compaction of the subfloor the acceleration increased to approximately 20 g. The initial crush acceleration peak, steady state crush response, and secondary peak towards the end of impact were all closely predicted by the simulation in terms of both acceleration magnitude and timing. These results provided additional confidence in using the developed model in predictive simulations for the infinity subfloor design.

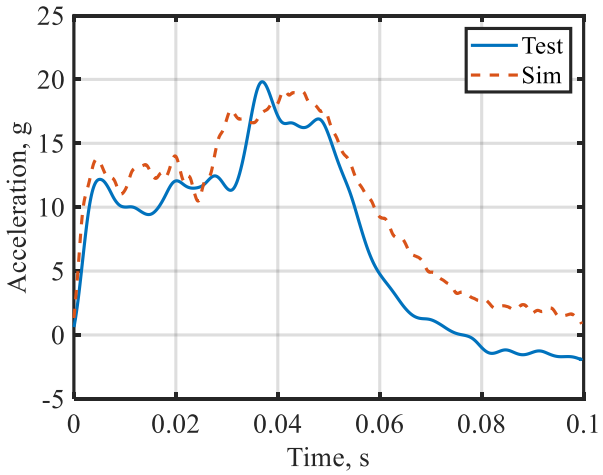

Figure 40. Correlation between measured and predicted impactor acceleration during vertical impact test with the “infinity” subfloor design

After verifying the EA response of the infinity subfloor at the component level, testing of the combined infinity subfloor and accordion crush tube seat EA system was conducted to verify the system level response of the combined EAs. Two vertical drop tower tests of the combined seat and subfloor EA were conducted with the Hybrid III 50th ATD seated in an aluminum seat bucket with a three-point belt. The EA seat and occupant system were mounted to the drop tower sled and dropped onto the infinity subfloor from a prescribed height selected for the desired impact velocity. The first test was conducted with an impact velocity of 20 ft/s and included a 4-layer infinity subfloor. The second test was conducted with an impact velocity of 26 ft/s and included a 5-layer infinity subfloor. Both conditions were replicated in simulation.

Test to simulation comparisons from each combined EA system test were made at the seat pan, ATD lumbar spine, and ATD upper neck and are shown in Figure 41. Both tests showed the combined EA system to effectively reduce occupant lumbar force well below the 1,500 lb. injury criteria limit, with a peak lumbar load of approximately 1,100 lb. being measured in both test conditions. The simulations of each test closely predicted peak, shape, and phasing of the acceleration time history measured at the seat pan, indicating the impact energy was accurately being transferred through both EA systems within the developed model. Accurate prediction of seat acceleration phasing also indicates that the timing of when EA crushing began and finished for both components was accurately captured by the model. The phasing and initial peak of the lumbar force was accurately predicted by the model. After the initial peak in lumbar force, the test response exhibited a sharp drop off followed by a lower rebound as the crush tube initiated and compacted.

However, the simulation showed only a slight drop in force as the crush tube initiated and it did not develop in the same way as that observed in the test. Although the full shape of the lumbar force response was not perfectly predicted, peak force and phasing in both test conditions were accurately captured. The upper neck force was effectively predicted by simulation in phase, shape, and peak values for both test conditions. The response drop-off after the EA tube initiation was better predicted in the ATD upper neck force than in the lumbar force. A secondary peak occurred in upper neck force in both test conditions, this response was identified in both models, though the peak was better captured in the 26 ft/s condition. Overall, the test results verified the occupant protection capabilities of the combined EA system. Additionally, the capability of the generated model to accurately predict seat, peak acceleration, lumbar force, and upper neck force provides confidence in its ability to effectively characterize the transfer of impact energy through the EA systems and occupant surrogate.

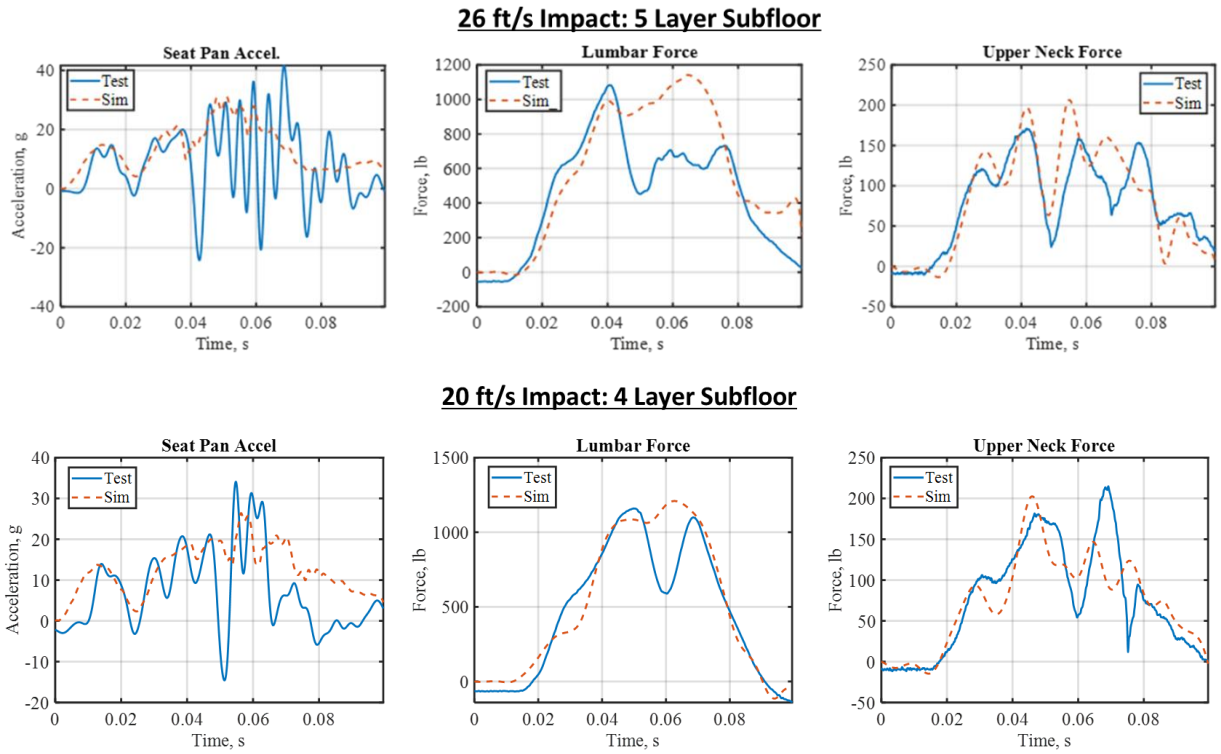

Figure 41. Correlation between test and simulation responses during the combined EA system drop testing.

The majority of impact conditions assessed up until this point utilize an impact velocity of 26 ft/s or below. These conditions were selected based on estimated vehicle vertical velocity during a 30 ft/s crash after the landing gear has absorbed a portion of the impact energy. To assess the capability of the combined EA system to further improve occupant safety, a final verification assessment was conducted with an impact velocity of 30 ft/s. This last assessment assumes that the vehicle structure provides no energy absorption during impact, thus making it a conservative demonstration of occupant safety capability independent from vehicle design. The effectiveness of the EA system to prevent injury, independently from vehicle design,

is important for potential use within eVTOL designs which encompass a broad range of shapes, unique structural materials, and types of landing gear. The 30 ft/s impact condition was assessed similarly to the previous drop tests of the combined EA system, in which a 50th percentile Hybrid III ATD was seated in an aluminum seat bucket with the accordion crush tube EA system on the seat rails. The seat and ATD were dropped onto the infinity subfloor from a prescribed height in order to produce the 30 ft/s impact velocity with the subfloor. The lumbar load response measured in this test and that predicted by simulation are shown in Figure 42**Error! Reference source not found.**. The peak lumbar load measured in this condition reached approximately 1,200 lb in both test and simulation demonstration an effective protection of the occupant lumbar spine through the use of the combined EA system in the 30 ft/s direct impact. Lumbar force reached just under this value at the initiation of the subfloor EA and then remained consistent throughout the compaction of both EA systems indicating a near optimal crush efficiency for the total EA system. The simulation closely matched the shape and phasing of the response indicating effective predictive capability for the developed EA system as well.

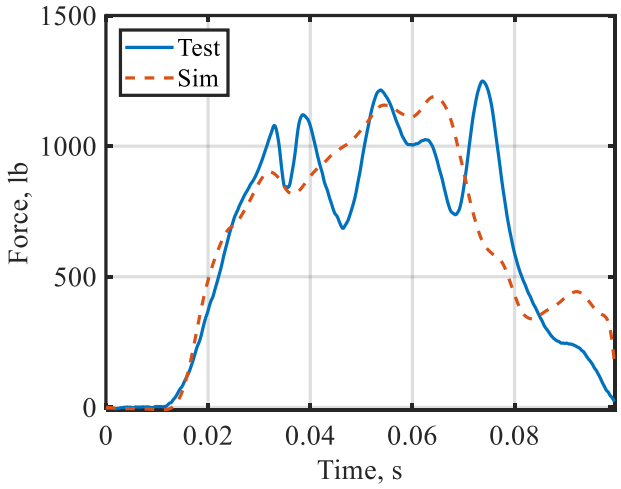

Figure 42. Test measured and simulation predicted lumbar load response in the 30 ft/s vertical impact with combined EA system.

7 Conclusions

The development of a new type of transport system like eVTOL vehicles comes with opportunities to improve and reshape technologies used in structural design for occupant protection. The current study aimed to develop an EA system tailored to the design priorities of eVTOL vehicles, namely in being lightweight and self-supporting so as to be independent from the design of the aircraft structure. The EA system also aimed to provide optimal EA response to minimize accelerative loading of occupants within a vehicle while also minimizing the stroke length of the EA. This study also developed EA design and analysis methodologies which could be applied to future EA system efforts across various design spaces.

First the material to be used within the EA components was selected. Material selection was made based on the criteria that the material needed to be both light weight and ductile while also having enough strength to maintain its structure during off-axis loading events. A selection of carbon fiber based composite

materials were evaluated for this purpose due to their high strength to weight ratios. The first material evaluated was a full-carbon fabric material which demonstrated a high-strength to weight ratio but had poor ductility, required a crush initiation force much higher than that measured during crushing, and exhibited material tearing during crush which resulted in inconsistent results with this material. The second material evaluated was a carbon-Kevlar fabric which had high ductility, high-strength to weight ratio, minimal crush initiation force, and consistent fold-based crush response. The final material evaluated was ultra-high molecular weight polyethylene and carbon fabric which also had high ductility and decent strength to weight ratio but produced an inconsistent crush response across the tests conducted. The carbon-Kevlar fabric was ultimately selected as the material to be used in the EA system development due to its consistent crush response, minimal crush initiation force and high-strength to weight ratio.

After selecting the material to be used in the EA system, the form of the EA components had to be determined. Two forms of EAs were selected for use: the first was a composite crush tube which could be used within a seat-based EA system, the second was a subfloor which was designed to operate independently from an aircraft structure to reduce impact energy transferred to the seat itself. Both EA components aligned to limit the vertical impact energy transferred to a seated occupant in order to reduce vertical lumbar compression to below regulatory limits during a crash event.

With the material and types of the EA components selected, the geometry of each EA component was then optimized for EA efficiency within the design space. First, the EA tube wall geometry was optimized using LS-Dyna simulations, leading to the selection of an accordion wall shape which produced a consistent folding crush response with a steady state crush force approaching that which was required for crush initiation. The results of the analytical optimization were verified through the fabrication and test of components under both static and dynamic environments. The EA crush tubes were then integrated into a seating system and tested using ATDs in a dynamic vertical drop tower test. The results demonstrated the effectiveness of the developed EA crush tubes to significantly reduce lumbar loads across a range of occupant sizes compared to a rigid seat design. The capability of this EA design was ultimately verified in a full-scale crash test of a representative fuselage airframe. In this test, the ATD in an EA crush tube seat system experienced measured lumbar load over 1,000 lb. less than the ATD in a rigid seat, resulting in lumbar loads below FAA certification limits. These results demonstrated the ability of an analytically optimized composite crush tube with a simple and lightweight design to effectively improve occupant safety within an eVTOL vehicle.

The lessons learned from optimizing the EA crush tubes were then applied to developing an EA subfloor. The primary goal of the subfloor design was to effectively reduce impact energy measured at the floor level in various levels of off-axis impact loading with a self-supporting component, independent from the vehicle structure. To this end, the first subfloor EA design was a boxed-cruciform shape which was exceptionally robust to off-axis loading and maintained its form during crushing without need for outside support. This design was effective in component level simulation and testing but ultimately proved to be too rigid when combined with the crush tube EA in the system level full-scale crash test evaluation. To optimize the complete EA system (seat and subfloor), the subfloor shape was redesigned to an infinity shape which retained horizontal and lateral rigidity but removed the wall intersection in the boxed-cruciform design which had produced a stiffness concentration.

The new infinity subfloor design was optimized in conjunction with the seat EA system in order to develop a subfloor which worked synergistically with the seat EA to further reduce occupant loads. This optimization was first done through LS-Dyna simulation and then validated through test. The final test of this system was a 30 ft/s impact of the EA seat with a 50th percentile ATD onto the subfloor EA. This test represented a 30 ft/s crash scenario not taking into account any external energy absorption by the vehicle structure. The combined EA system limited lumbar force to approximately 1,200 lb., which is below the FAA certification limit. These results demonstrated that a lightweight EA system designed to act independent of future aircraft vehicle structural designs can effectively limit occupant injury risk in severe but survivable crash conditions.

This study demonstrated an effective methodology of using analysis supported by test to develop EA systems, independent from vehicle architecture, that are capable of reducing occupant injury risk in aerospace vehicles. The EA systems presented here provide reference for the development of new technologies to improve occupant safety within advancing fields of aerospace transport such as those being brought on through eVTOL vehicle designs. Occupant safety will always be essential to the adoption of any new form of transportation and new EA technologies will be key to ensuring safe and reliable transportation in the future

8 References

1. Kellas, S., and Jackson, K.E., "Deployable System for Crash-Load Attenuation," Proceedings of the 63rd AHS Annual Forum, Virginia Beach, VA, May 1-3, 2007.

2. Littell, J. D., Jackson, K. E., Annett, M. S., Seal, M. D., Fasanella, E. L. "The development of two composite energy absorbers for use in a transport rotorcraft airframe crash testbed (TRACT 2) full-scale crash test." Proceedings from the 71st American Helicopter Society Annual Forum and Technology Display. Virginia Beach, VA, May 5-6, 2015.

3. Federal Aviation Administration. "Emergency Landing Dynamic Conditions." 14 CFR § 27.562. Amended November 13, 1989.

4. Federal Aviation Administration. "Emergency Landing Dynamic Conditions." 14 CFR § 23.562. Amended December 2, 2011.

5. LS-DYNA Aerospace Working Group, "Modeling Guidelines Document v.22-1." June 2022.

6. Littell, J.D. "The Development of a Conical Composite Energy Absorber for use in the Attenuation of Crash/Impact Loads". Paper/presentation at the American Society of Composites 29th Annual Conference, San Diego CA. September 8-10, 2014.

7. American Society for Testing and Materials. "Standard Test Method for In-Plane Shear Response of Polymer Matrix Composite Materials by Tensile Test of a ±45° Composite." ASTM-D3518M. 2013.

8. Littell, J. and Putnam, J., "The Evaluation of Composite Energy Absorbers for use in UAM VTOL Vehicle Impact Attenuation". Proceedings from the 75th American Helicopter Society Annual Forum and Technology Display. Philadelphia, PA. May 13-16, 2019.

9. Jackson, K.E., Fasanella, E.L., and Littell, J.D. "Development of a Continuum Damage Mechanics Material Model of a Graphite-Kevlar ® Hybrid Fabric for Simulation the Impact Response of Energy Absorbing Subfloor Concepts." Proceedings from the 73rd Annual American Helicopter Society Annual Forum and Technology Display. Fort Worth, TX. May 9-11, 2017.

10. Putnam, J.B. and Littell, J.D. "Crashworthiness of a Lift plus Cruise eVTOL Vehicle Design within Dynamic Loading Environments." Proceedings from the Vertical Flight Society 76th Annual Forum and Technology Display. October 5-8, 2020.

11. Littell, J., Putnam, J.B., Gardner, N.W., Hardy, R.C., "A Summary of Results from Vertical Drop Testing of Hybrid III and WIAMan ATDs." NASA/TM-2015-20250000911. November 1, 2015.

12. Putnam, J.B., Littell, J.D., Gardner, N., Mennu, M., "Component Characterization of an eVTOL Reference Model for Crashworthiness Studies," Proceedings from the Vertical Flight Society 80th Annual Forum and Technology Display, May 7-9, 2024.

13. Jones, N.L., Putnam, J.B., Untaroiu, C., "Study of Advanced Occupant Models to Quantify Injury Risk for eVTOL Vehicles." Journal of the American Helicopter Society, Vol. 70, 2025.

14. Putnam, J.B., Littell, J.D., Reaves, M., "Development and Analysis of Energy Absorbing Subfloor Concepts to Improve eVTOL Crashworthiness," Proceedings from the Vertical Flight Society 78th Annual Forum and Technology Display, Fort Worth, TX. May 2022.

15. Littell, J.D., Putnam, J.B., Cooper, M., "Simulation of Lift plus Cruise Vehicle Models to Define a Full-Scale Crash Test Campaign," Proceedings from the Vertical Flight Society 77th Annual Forum and Technology Display, May 12, 2022

16. Putnam, J.B., Littell, J.D., "Simulation and Analysis of NASA Lift Plus Cruise eVTOL Crash Test," Proceedings from the Vertical Flight Society 79th Annual Forum and Technology Display, May 16-18, 2023.

17. Silva, C., Johnson, W., Antcliff, K.R., Patterson, M.D., "VTOL Urban Air Mobility Concept Vehicles for Technology Development," Proceedings from the 2018 Aviation Technology, Integration, and Operations Conference, Atlanta, GA, June-25-29, 2018.

18. Littell, J.D., Putnam, J.B., "A Summary of Test Results from a NASA Lift + Cruise eVTOL Crash Test," Proceedings from the Vertical Flight Society 79th Annual Forum and Technology Display, May 16-18, 2023.